J Neurophysiol 117: 1894–1910, 2017.
First published February 15, 2017; doi:10.1152/jn.00811.2016.

RESEARCH ARTICLE | *Control of Movement*

Alteration of the microsaccadic velocity-amplitude main sequence relationship after visual transients: implications for models of saccade control

Antimo Buonocore,[1,3] Chih-Yang Chen,[1,2,3] Xiaoguang Tian,[1,2,3] Saad Idrees,[1,2] Thomas A. Münch,[1] and Ziad M. Hafed[1,3]

[1]*Werner Reichardt Centre for Integrative Neuroscience, Tübingen University, Tübingen, Germany;* [2]*Graduate School of Neural and Behavioural Sciences, International Max Planck Research School, Tübingen University, Tübingen, Germany; and* [3]*Hertie Institute for Clinical Brain Research, Tübingen University, Tübingen, Germany*

Submitted 13 October 2016; accepted in final form 14 February 2017

Buonocore A, Chen CY, Tian X, Idrees S, Münch TA, Hafed ZM. Alteration of the microsaccadic velocity-amplitude main sequence relationship after visual transients: implications for models of saccade control. *J Neurophysiol* 117: 1894–1910, 2017. First published February 15, 2017; doi:10.1152/jn.00811.2016.—Microsaccades occur during gaze fixation to correct for miniscule foveal motor errors. The mechanisms governing such fine oculomotor control are still not fully understood. In this study, we explored microsaccade control by analyzing the impacts of transient visual stimuli on these movements' kinematics. We found that such kinematics can be altered in systematic ways depending on the timing and spatial geometry of visual transients relative to the movement goals. In two male rhesus macaques, we presented peripheral or foveal visual transients during an otherwise stable period of fixation. Such transients resulted in well-known reductions in microsaccade frequency, and our goal was to investigate whether microsaccade kinematics would additionally be altered. We found that both microsaccade timing and amplitude were modulated by the visual transients, and in predictable manners by these transients' timing and geometry. Interestingly, modulations in the peak velocity of the same movements were not proportional to the observed amplitude modulations, suggesting a violation of the well-known "main sequence" relationship between microsaccade amplitude and peak velocity. We hypothesize that visual stimulation during movement preparation affects not only the saccadic "Go" system driving eye movements but also a "Pause" system inhibiting them. If the Pause system happens to be already turned off despite the new visual input, movement kinematics can be altered by the readout of additional visually evoked spikes in the Go system coding for the flash location. Our results demonstrate precise control over individual microscopic saccades and provide testable hypotheses for mechanisms of saccade control in general.

NEW & NOTEWORTHY Microsaccadic eye movements play an important role in several aspects of visual perception and cognition. However, the mechanisms for microsaccade control are still not fully understood. We found that microsaccade kinematics can be altered in a systematic manner by visual transients, revealing a previously unappreciated and exquisite level of control by the oculomotor system of even the smallest saccades. Our results suggest precise temporal interaction between visual, motor, and inhibitory signals in microsaccade control.

Address for reprint requests and other correspondence: A. Buonocore, Werner Reichardt Centre for Integrative Neuroscience, Otfried-Mueller Str. 25, Tübingen 72076, Germany (e-mail: antimo.buonocore@cin.uni-tuebingen.de).

microsaccades; saccades; saccadic inhibition; superior colliculus; omnipause neurons

SACCADES PLAY AN IMPORTANT ROLE in visual perception by rapidly realigning the fovea with objects in the environment. Though the mechanisms of saccade control have been a mainstay of research for several decades (Hafed 2016), important questions remain ripe for further mechanistic understanding. Among these, interactions between the decision to move the eyes and inhibitory processes that help maintain fixation are particularly intriguing, especially in light of the implications of eye movement generation on the stream of visual information arriving from the retina.

In this study, we focused on a phenomenon in which visual transients result in a strong, yet short-lived, decrease in saccade (Buonocore and McIntosh 2008; Reingold and Stampe 1999, 2000, 2002) or microsaccade probability (Engbert and Kliegl 2003; Hafed and Clark 2002; Hafed and Ignashchenkova 2013; Hafed et al. 2011, 2013; Peel et al. 2016; Rolfs et al. 2008). Several hypotheses about such "saccadic inhibition" have been proposed, but they all generally revolve around the idea of lateral inhibition between the location of the so-called "distracting" flash and the location of the saccade goal (Bompas and Sumner 2011; Buonocore and McIntosh 2008; Edelman and Xu 2009; Reingold and Stampe 2000, 2002). In line with this, superior colliculus (SC) neurons encoding saccade goal location experience a rapid and transient reduction in presaccadic buildup activity when a remote "distractor" is flashed (Dorris et al. 2007). Such reduction is often credited with increasing saccadic reaction times (RT), causing a characteristic "dip" in the overall RT distribution after flash onset (i.e., saccadic inhibition) (Bompas and Sumner 2011; Buonocore and McIntosh 2008, 2012; Edelman and Xu 2009).

However, saccadic inhibition is a more nuanced phenomenon. At the onset and trough of RT distribution dips, saccades can and still do occur. These saccades are special because of at least two reasons. First, they happen near the time at which transient SC activity reduction would be expected to happen to mediate saccadic inhibition; that is, for these specific movements, the transient activity dip is replaced with a movement burst instead. Second, the time of occurrence of these saccades

after flash onset is usually less than the so-called "point of no return," or the point (~60 ms before movement onset) after which the flash presumably cannot alter the motor plan (Findlay and Harris 1984; Ludwig et al. 2007). Recent results (Buonocore et al. 2016; Edelman and Xu 2009; Guillaume 2012) have shown that saccade kinematics can indeed be altered beyond the point of no return: saccades may appear truncated (as shown schematically in Fig. 1*A*) and thus violate the well-known velocity-amplitude main sequence relationship (Bahill et al. 1975; Zuber et al. 1965). One common hypothesis (Buonocore et al. 2016; Edelman and Xu 2009; Guillaume 2012) for this violation is that an ongoing saccade is interrupted: the observed peak velocity reflects that of the planned movement, whereas the amplitude reflects that of the truncated one.

In the present study, we investigated an additional potential mechanism for the kinematic alteration schematized in Fig. 1*A*, which we believe can illuminate broader phenomena of saccade/microsaccade triggering and inhibition. At the heart of this mechanism is the idea that flash onset induces visual responses (i.e., activity increases) in the SC and other spatially organized oculomotor structures shortly after the onset (Fig. 1*B*). Now, if brain stem omnipause neurons (OPNs), which are thought to help gate saccades (Keller 1974; Moschovakis et al. 1996; Scudder et al. 2002), were to pause their activity shortly after flash onset for whatever reason, then saccade bursts would occur in the SC at the goal location instead of the activity reductions that would take place if the saccade was successfully delayed. Critically, these saccade bursts would also be temporally coincident with spatially dissociated visual bursts induced by the recently occurring flash onset. As a result, readout of spatial maps at saccade onset would reveal spiking activity not only at the saccade goal location but also at the flash location (Fig. 1, *B* and *C*). Given the spatial arrangement of flashes typically employed in some of these experiments (e.g., Fig. 1*A*), such spatial readout may result in shorter saccades than originally planned (Fig. 1*C*). In this case, the kinematic alteration in Fig. 1*A* would be one of an altered spatial drive to the saccade itself, rather than (or in addition to) an interruption of an ongoing triggered one.

We tested behavioral predictions of this potential mechanism by showing that main sequence violations also can occur in the opposite direction from that shown in Fig. 1*A* (i.e., with higher rather than lower saccade amplitudes after flash onset). We did this by exploiting microsaccades, for which the motor goal is foveal and flashes can be more eccentric, resulting in different spatial readout from that in Fig. 1*C*. Besides suggesting additional important mechanisms for interpreting saccadic inhibition phenomena in general, our results show for the first time that microsaccade kinematics can be significantly altered. This demonstrates a previously unappreciated and exquisite level of control by the oculomotor system of the smallest possible saccades.

MATERIALS AND METHODS

Animal Preparation and Laboratory Setup

We collected behavioral data from two (P and N) adult, male rhesus monkeys (*Macaca mulatta*) that were 6–10 yr of age and weighed 6–13 kg. All experimental protocols for the monkeys were in accordance with the guidelines for animal experimentation approved by the Regierungspräsidium of Tübingen, Germany. The monkeys were prepared using standard surgical techniques necessary for behavioral training and neurophysiological investigations, as described previously (Chen and Hafed 2013; Chen et al. 2015; Hafed and Chen 2016). We used a custom-built experimental control system that drove stimulus presentation and ensured monkey behavioral monitoring and

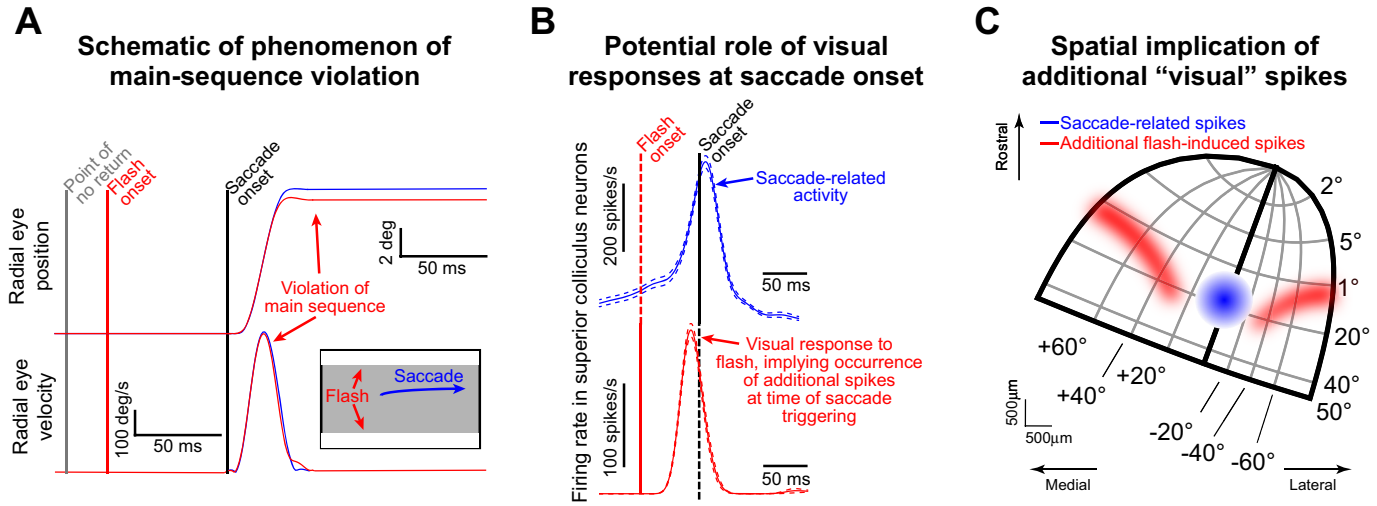

Fig. 1. The phenomenon of kinematic alteration. *A*: schematic of the phenomenon from a typical scenario from the literature (Buonocore et al. 2016; Reingold and Stampe 2002). *Top* panel shows radial eye position for 2 hypothetical saccades. In blue, the saccade is triggered without a preceding visual flash; in red, a flash consisting of 2 horizontal full-screen white bars (see *inset*) appears right before saccade onset and after the point of no return (gray vertical line). The saccade amplitudes are different even though peak velocity (shown in *bottom* panel) is minimally affected. Thus the post-flash saccade violates the main sequence relationship and has different kinematics from the no-flash movement. Note how eye velocity decelerates slightly faster for the post-flash saccade compared with the no-flash saccade, contributing to the reduced amplitude in the former movement. *B*: in this study, we were interested in the role of flash-induced visual responses in spatial structures such as the superior colliculus (SC). If the post-flash saccade is triggered at the time of visual response occurrence, then readout of spatial maps would have access not only to the saccade-related spikes (blue) but also to the visual spikes. *C*: spatially, the visual spikes would alter the center of mass of activity being read out by the oculomotor system to specify saccade end point. In this example, the SC map (Hafed and Chen 2016) would have a center of mass less eccentric than the blue saccade-related burst, which could explain the lower saccade amplitude in *A*. We explored the implications of this mechanism in this study.

reward delivery, as detailed elsewhere (Chen and Hafed 2013; Tian et al. 2016).

Behavioral Tasks

In all of our tasks, the monkeys generated normal saccadic or microsaccadic behavior expected from the particular stimulus scenarios that we employed, and we simply introduced a transient or sustained visual "flash" of different properties at a random time. We then analyzed the metrics and kinematics of the saccades that were generated shortly after flash onset (i.e., those near the expected "saccadic inhibition" period). As we describe below in more detail, the majority of our experiments exploited microsaccades, because they are very small in amplitude (e.g., see Figs. 2*A* and 3 in RESULTS) while at the same time being governed by neural mechanisms similar to those of much larger saccades (Chen and Hafed 2017; Hafed 2011; Hafed et al. 2009, 2015; Hafed and Krauzlis 2010, 2012; Peel et al. 2016). This was important because it allowed us to present flashes that would alter readout of spatial maps in a manner opposite that of Fig. 1*C* (*experiment 1*); for example, with a flash location much more eccentric than the saccade goal location (e.g., see Fig. 2*B* in RESULTS). Additionally, exploiting microsaccades allowed us to explore cases in which the flash and the movement goal would be extremely close to each other, and on the scale of individual minutes of arc (*experiment 2*). This revealed a remarkable universality of the phenomenon of saccadic inhibition and its associated kinematic alterations of saccades and microsaccades that we describe in this article, even when the saccade goal and the "distracting flash" are virtually colocalized (see RESULTS).

Experiment 1: Microsaccades and peripheral flashes. The purpose of this task was to demonstrate that both saccade amplitude increases and decreases can occur during saccadic inhibition, and even within the same task. To do this, we presented a flash more eccentric than the saccade goal, which in this experiment was at a tiny eccentricity because we focused on microsaccades. This task was the same as that used in the subset of experiments presented in Tian et al. (2016) that were performed by monkeys. In fact, we reanalyzed the same data set from the control condition of their experiments (see their Fig. 10*B*), especially because the task was ideally suited for our current purposes of having a flash more eccentric than the movement goal (e.g., see Fig. 2*B*). Briefly, monkeys fixated a small, white fixation spot presented over a gray background for 400–900 ms. A peripheral white target (which served as our peripheral "flash" stimulus in the present context) then appeared at 5° eccentricity either horizontally or vertically, and it persisted for >750 ms (Tian et al. 2016). The monkeys' task was to maintain fixation until removal of the fixation spot (Tian et al. 2016). In this experiment, we analyzed only the microsaccades occurring near flash onset, because this is when microsaccadic inhibition was expected to take place (Hafed and Ignashchenkova 2013), as we also have confirmed in RESULTS. In addition to microsaccade rate, we also analyzed microsaccade peak velocity and amplitude, which were not reported in Tian et al. (2016). It should be noted that in Tian et al. (2016), some trials with retinal image stabilization were randomly interleaved in the same sessions to investigate other issues, but these were not analyzed in this work. We are confident that the interleaved trials do not affect our conclusions in this study, especially because similar results from the same two animals were seen with reanalysis of another data set (Hafed and Ignashchenkova 2013) involving peripheral flashes but without interleaved retinal image stabilization trials (data not shown).

Experiment 2: Microsaccades and foveal flashes. The purpose of this task was to explore how close the flash can be to the eye movement goal and still generate saccadic inhibition and kinematic alterations. Specifically, interpretations like those based on the study of Dorris et al. (2007) might suggest that flashes need to be remote from the saccade goal to generate saccadic inhibition (hence, the use of the phrase "remote distractor effect" in some terminology; Walker et al. 1997). Therefore, we exploited the fact that microsaccades correct minute eye position errors from the foveal fixation spot (Guerrasio et al. 2010; Ko et al. 2010; Tian et al. 2016), and we placed the flash exactly on the spot. In this case, the flash location (at the fixation spot) is very close to the goal location for the great majority of microsaccades (as we confirm in Figs. 5*C* and 7*B*, and with microsaccade amplitude histograms in Figs. 2*A* and 6*B*). Monkeys fixated the same white fixation spot for 400–1,000 ms, after which we transiently dimmed the spot to black and then back to white after ~50 ms. We looked for signatures of microsaccadic inhibition in this paradigm, and also for alterations in microsaccade kinematics as predicted from *experiment 1* above (see *Data Analysis* below).

Experiment 3: Large saccades and full-screen flashes. To confirm that monkeys can exhibit alterations in saccade kinematics for large saccades, as shown in previous experiments in humans (Buonocore et al. 2016; Edelman and Xu 2009; Guillaume 2012), and not just for microsaccades, we tested one of our monkeys (*monkey N*) with a free-viewing task. The monkey viewed a cloud pattern (e.g., see Fig. 9 in RESULTS) for 0.4–1.7 s per trial. The pattern was generated as follows. A checkerboard pattern of randomly placed white and black squares was blurred with a two-dimensional Gaussian blurring filter (see Fig. 9*A*). For each image, the size of the squares and the σ parameter of the Gaussian filter were chosen from four possible values each, to generate four possible spatial scales of the cloud pattern, which were randomly interleaved across trials. The spatial scales were included for other experimental purposes, and they are irrelevant for the present analyses. During viewing of the cloud pattern, and at a random time ~200–1,200 ms after trial onset, the entire screen was turned either black or white for ~16 ms, which was sufficient to cause saccadic inhibition (see RESULTS). We analyzed alterations in the kinematics of the free-viewing saccades that the monkey was generating during this task (i.e., after flash onset and near the saccadic inhibition period), to confirm that monkeys can exhibit the large-saccade kinematic changes that have previously been reported only in humans (Buonocore et al. 2016; Edelman and Xu 2009; Guillaume 2012).

Data Analysis

Eye movement analyses. We detected saccades and microsaccades using our previous methods (Chen and Hafed 2013; Hafed et al. 2009), and we manually inspected all data to correct for any false alarms or misses. Briefly, we detected movement onset and end on the basis of eye velocity and acceleration criteria. We first estimated eye velocity and acceleration from the measured eye position values, which were sampled at 1 kHz. We differentiated horizontal and vertical eye position, using a smoothing differentiation digital filter, to obtain horizontal and vertical eye velocity. We then obtained radial eye velocity from the horizontal and vertical eye velocities before differentiating once again to obtain radial eye acceleration. We set a radial eye velocity threshold above eye tracker noise levels and flagged all points above this threshold as being part of a microsaccade or saccade. We then marched backward in time from the first detected sample until radial eye acceleration decreased below an acceleration threshold; this allowed us to refine our estimate of movement onset. Similarly, we marched forward in time from the last detected sample until radial eye acceleration decreased below the same acceleration threshold; this allowed us to refine our estimate of movement end. Thus movement onset and end were computed on the basis of a combination of velocity and acceleration criteria.

After detecting microsaccade or saccade onset and end, we defined movement radial amplitude as the Euclidean distance between eye position at movement onset and eye position at movement end. We defined movement direction as the arctangent subtended by the horizontal and vertical eye displacements between movement onset and end. For example, a movement to the right and up would have a positive horizontal and vertical displacement. The amplitude is the

radial distance of the two displacements, and the direction is the arctangent of the ratio of vertical to horizontal displacement.

When we plotted "radial eye position" traces for saccades or microsaccades in our figures (e.g., see Fig. 3), we plotted the Euclidean distance of any eye position sample during a given movement (i.e., at any given millisecond of time) from the eye position that was observed at saccade or microsaccade onset. In other words, the radial eye position during a movement is the distance that the eye had traversed from its position at movement onset. The advantage of using this way of plotting saccades and microsaccades is that it allows us to plot a single trace to demonstrate saccade or microsaccade amplitude, instead of having to plot two traces (one for horizontal eye position and one for vertical eye position; Hafed et al. 2009).

It should be noted that our smoothing digital differentiation filter introduces some ripples in eye velocity traces near the noise limit of the eye tracker (e.g., see the small radial eye velocity undulations during the fixation periods surrounding the example microsaccades of Fig. 3). This is expected out of filtering, which is needed to regularize the differentiation operation. However, it does mean that inspection of overall velocity trajectories (as opposed to only peak velocities) is more reliable when done for average traces of multiple movements (e.g., see Figs. 4 and 10) as opposed to individual movements (e.g., see Fig. 3). The reason that we included individual traces (e.g., see Fig. 3) was that we wanted to demonstrate the robustness of the mismatches between amplitude and peak velocity that we report in this study, even for individual tiny microsaccades.

Experiment 1: Microsaccades and peripheral flashes. We classified each individual microsaccade in a trial as having a direction within ±45° from either the location of the peripheral stimulus (our "toward" condition) or the location opposite from the peripheral stimulus (our "opposite" condition). Microsaccades of other directions were not further analyzed in this study, but these were less frequent anyway given the dependence of microsaccade directions on peripheral stimuli (Engbert and Kliegl 2003; Hafed and Clark 2002; Hafed and Ignashchenkova 2013; Tian et al. 2016). For example, during the interval 40–100 ms after peripheral stimulus onset (see Fig. 2, *C–E*), 59.2% of all microsaccades were either toward or opposite movements, and 40.8% were in other directions ($P < 0.01$, Binomial distribution fits).

In addition to analyzing the time course of microsaccade rate as a function of time relative to peripheral stimulus onset, we also analyzed the time courses of microsaccade amplitude and peak velocity for either toward or opposite microsaccades. We used running averages with a window of 50 ms and steps of 5 ms. On the basis of the microsaccade rate time course, we identified a period of inhibition (40–100 ms after stimulus onset in this experiment; see RESULTS) during which we compared microsaccade kinematics for toward and opposite microsaccades. To do the latter, we matched microsaccades during the inhibition period for either amplitude or peak velocity, and we checked whether peak velocity or amplitude, respectively, was matched or not. For example, if toward microsaccades were matched in amplitude to opposite microsaccades and their peak velocities were different, then this meant an alteration of microsaccade kinematics between toward and opposite movements. To demonstrate the generality of our results, we also plotted the ratio of peak velocity (in °/s) to movement amplitude (in degrees) for toward and opposite microsaccades independently of amplitude or peak velocity. Because the main sequence relationship is monotonic and well behaved (Bahill et al. 1975; Zuber et al. 1965), this ratio is relatively constant for a large dynamic range of movement amplitudes. If the ratio is altered near microsaccadic inhibition, then this suggests an alteration in the main sequence, or microsaccade kinematics, as we show in RESULTS.

Experiment 2: Microsaccades and foveal flashes. We first checked the directions and end points of microsaccades relative to the foveal flash location (i.e., the location of the dimming fixation spot) to confirm that microsaccades toward the fixation spot tend to be goal-directed and reduce foveal motor errors (Tian et al. 2016). If that is the case, then a foveal flash for a microsaccade toward the fixation spot is conceptually similar to a peripheral flash in the same direction as a microsaccade (see Fig. 2*B*, *top*), except that the foveal flash would be happening near the movement goal, and similarly for opposite microsaccades. Therefore, we classified microsaccade directions as follows: toward microsaccades were defined as those with a direction within ±30° from the axis connecting the foveal flash location and the starting position of the eye; opposite microsaccades were defined as those with directions within ±30° from the axis connecting the foveal flash location and the starting position of the eye movement. For all such microsaccades occurring from −150 to 50 ms relative to flash onset (i.e., during a baseline fixation interval and before the onset of microsaccadic inhibition), we plotted the ending eye position after a given microsaccade. If the ending position was closer to the fixation spot than the starting position of the microsaccade, then the microsaccade was error reducing; if the ending position was farther, then the microsaccade was error increasing (see Fig. 5 in RESULTS). Similar results were also observed during the inhibition period (e.g., see Fig. 7*B*).

For summarizing alterations of microsaccadic kinematics near the inhibition period after flash onset, we computed time courses of microsaccade rate, amplitude, peak velocity, and peak velocity to amplitude ratio in this experiment. We used binning procedures similar to those used for the peripheral flash experiment mentioned above.

We also summarized alterations in microsaccade kinematics across all trials by directly analyzing main sequence curves. We first estimated the "baseline" velocity-amplitude main sequence from all microsaccades occurring 0–150 ms before flash onset. We plotted peak velocity against microsaccade amplitude and fitted the data using linear regression (Buonocore et al. 2016), and we obtained 95% confidence intervals around the fits. We then took the time course curves of microsaccade amplitude and peak velocity 5–205 ms after flash onset (i.e., around the period of inhibition), and we plotted them as a phase-plane curve in velocity-vs.-amplitude space (e.g., see Fig. 7*C* in RESULTS). If the kinematics of microsaccades are altered near the time of microsaccadic inhibition, then the curve for microsaccades occurring near the inhibition period should deviate away from the baseline main sequence curve, as we show in RESULTS.

We also summarized kinematic alterations as a function of microsaccade amplitude. We used the analysis technique of Buonocore et al. (2016) to obtain a "kinematic alteration" index, which is essentially a normalized peak velocity, and we plotted this index as a function of microsaccade radial amplitude for microsaccades occurring near the inhibition period. Briefly, the index was obtained using the following procedure. First, for an observed microsaccade amplitude, we derived the predicted peak velocity by using the coefficients extracted from the linear regression described above. Second, we divided the actual observed peak velocity by the predicted one for each of the microsaccades so that an index value of 1 means no alteration in microsaccade kinematics.

Because the great majority of microsaccades in this experiment were toward movements (see RESULTS and Tian et al. 2016), most analyses near the inhibition period for this experiment were only performed for toward microsaccades, to allow statistical confidence to be obtained. However, we inspected opposite results nonetheless, and we confirmed that they are qualitatively consistent with those obtained from *experiment 1* above.

Experiment 3: Large saccades and full-screen flashes. The monkey was freely scanning a cloud pattern (e.g., see Fig. 9A in RESULTS). If the monkey made saccades to locations near the corners of the display and the flash happened right before these saccades, then this is akin to the flash having a spatial center of mass less eccentric than the location of the saccade goal. Thus this scenario would allow us to replicate human experiments, but in monkeys, and to demonstrate that the microsaccade effects from the above experiments also generalize to larger saccades in monkeys. Therefore, we selected all saccades starting from one region of the display and ending in another region,

either in baseline (20–200 ms before flash onset) or around a saccadic inhibition period (0–200 ms after flash onset). The starting and ending regions were selected such that the saccade goal was always close to one corner of the entire flash (see Fig. 9*B* in RESULTS for the definition of the regions). It should be emphasized that even though the monkey was freely viewing, we selected saccades in the baseline and inhibition phases such that movements were matched for starting and ending regions of the display, allowing a fair comparison of kinematics between baseline and post-flash saccades. We then compared main sequence curves for the two groups of movements. Note that there were not sufficient saccades with end points such that the flash had a center of mass more eccentric than the end point of the saccade, so we did not analyze these movements. However, coarse inspection of these saccades revealed different kinematic patterns from the saccades that we did analyze (i.e., with the flash being predominantly less eccentric than the saccade goal), consistent with our microsaccade results.

Finally, in all figures in this article, we show 95% confidence intervals. For proportions, the 95% confidence intervals were estimated by fitting the observed proportion value (P) and number of observations (n) to a binomial distribution and then recovering the 95% intervals. For data with variance measurements, 95% confidence intervals were obtained as a multiple of the standard error value.

RESULTS

Microsaccade Amplitude Modulations as a Function of the Spatial Geometry of Visual Transients Relative to the Movement Goal

Presaccadic transient flashes like the example one shown in Fig. 1*A* often result in shorter saccadic amplitudes than normally expected from the observed peak velocity (Buonocore et al. 2016; Edelman and Xu 2009; Guillaume 2012). This could reflect some sort of "interruption" of a planned saccade, but it might also reflect an additional factor of spatial leakage of flash-induced spiking activity (e.g., in the SC) into downstream motor structures converting the spatial map representations into eye velocity commands (e.g., Fig. 1, *B* and *C*). Experimentally, a convenient means to demonstrate such an additional mechanism would be to study microsaccades, whose tiny size (Fig. 2*A*) confers the advantage that the movement goal can be quite foveal whereas the visual flash is much more eccentric. For example, in Fig. 2*B*, *top*, a microsaccade could be planned toward a near eccentricity in one direction (blue location of putative motor bursts in the SC), and a flash could occur in the same direction but at an eccentricity ~10–30 times larger (red location of a putative visual burst in the SC). In this case, if a microsaccade were to be triggered (blue) near the time of arrival of visual spikes associated with the flash onset (red), that is, near the time of "saccadic inhibition" (Fig. 1), then spatial readout of the map would result in a different microsaccade end point from that occurring without the flash. In this specific case (Fig. 2*B*, *top*), the microsaccade would be expected to increase in amplitude rather than decrease as in the schematic illustration of Fig. 1*A*.

Based on the prior literature on microsaccadic inhibition, some experiments have shown reductions in microsaccade amplitudes shortly after sensory transients (Rolfs et al. 2008), whereas others have shown increases (Hafed and Ignashchenkova 2013). According to our hypothesized mechanism of Fig. 1, *B* and *C*, these results, including those on large saccades in Fig. 1*A*, may potentially be reconciled when a framework including readout of spatial maps (e.g., from the SC) is considered. We demonstrated this with *experiment 1* (MATERIALS AND METHODS).

Across trials, the stimulus could appear before a microsaccade either in the same direction as the peripheral stimulus (Fig. 2*B*, *top*) or a microsaccade in the opposite direction (Fig. 2*B*, *bottom*). In both cases, peripheral stimulus onset caused robust microsaccadic inhibition (Fig. 2*C*), as expected. The likelihood of observing a microsaccade dropped to near-zero levels within <100 ms after stimulus onset before recovering soon after, which is a characteristic signature of saccadic and microsaccadic inhibition (Hafed and Ignashchenkova 2013; Reingold and Stampe 2002; Rolfs et al. 2008). Note that the postinhibition rebound in Fig. 2*C* was strongly different for toward or opposite microsaccades, but this is expected given that postinhibition microsaccade directions are typically heavily biased away from the stimulus location (Hafed and Ignashchenkova 2013; Tian et al. 2016). Importantly for the present study, the amplitudes of the few microsaccades that did occur near the inhibition period strongly depended on the direction of these microsaccades (Fig. 2*D*): for toward microsaccades, the few movements that did happen around the inhibition period (e.g., during the gray region in Fig. 2*D*) were significantly larger in amplitude than expected from microsaccades during fixation (compare with amplitude in the prestimulus interval during steady fixation); on the other hand, opposite microsaccades experienced a transient reduction in amplitude.

We confirmed these observations statistically; for all microsaccades occurring 40–100 ms after stimulus onset, we calculated microsaccade amplitudes for movements either toward or opposite the stimulus location. We also calculated amplitudes for toward and opposite movements occurring right before stimulus onset (specifically during the interval from −100 to −40 ms from stimulus onset). A 2 × 2 ANOVA (with one factor being direction, toward vs. opposite, and the other factor being time, before vs. after stimulus onset) revealed significant main and interaction effects ($P < 0.02$ for each effect). Post hoc Tukey-Kramer comparisons revealed that the effects were the result of microsaccade amplitudes during the inhibition interval being different between toward and opposite movements, and also being different from the amplitudes during the prestimulus interval. Specifically, during the inhibition period, average amplitude toward the stimulus location was 23.17 min arc, whereas average amplitude was 11.28 min arc for opposite movements ($P < 0.01$, Bonferroni corrected). Right before stimulus onset, the amplitudes of toward and opposite microsaccades were not statistically different (14.82 vs. 15.7 min arc, respectively; $P = 0.6763$). Similar observations were also made for microsaccade peak velocities (Fig. 2*E*).

Thus metric changes in saccade amplitude and peak velocity are not necessarily restricted to amplitude reductions as in Fig. 1*A* and Rolfs et al. (2008), but they can also involve both amplitude increases and decreases depending on the spatial layout of the stimulus flash relative to the planned movement goal location at the time of saccade triggering.

Kinematic Alterations in Microsaccades After Peripheral Flash Onset

In addition to amplitude differences, the kinematics of toward and opposite microsaccades in the same experiment of Fig. 2 were also different from each other near the inhibition

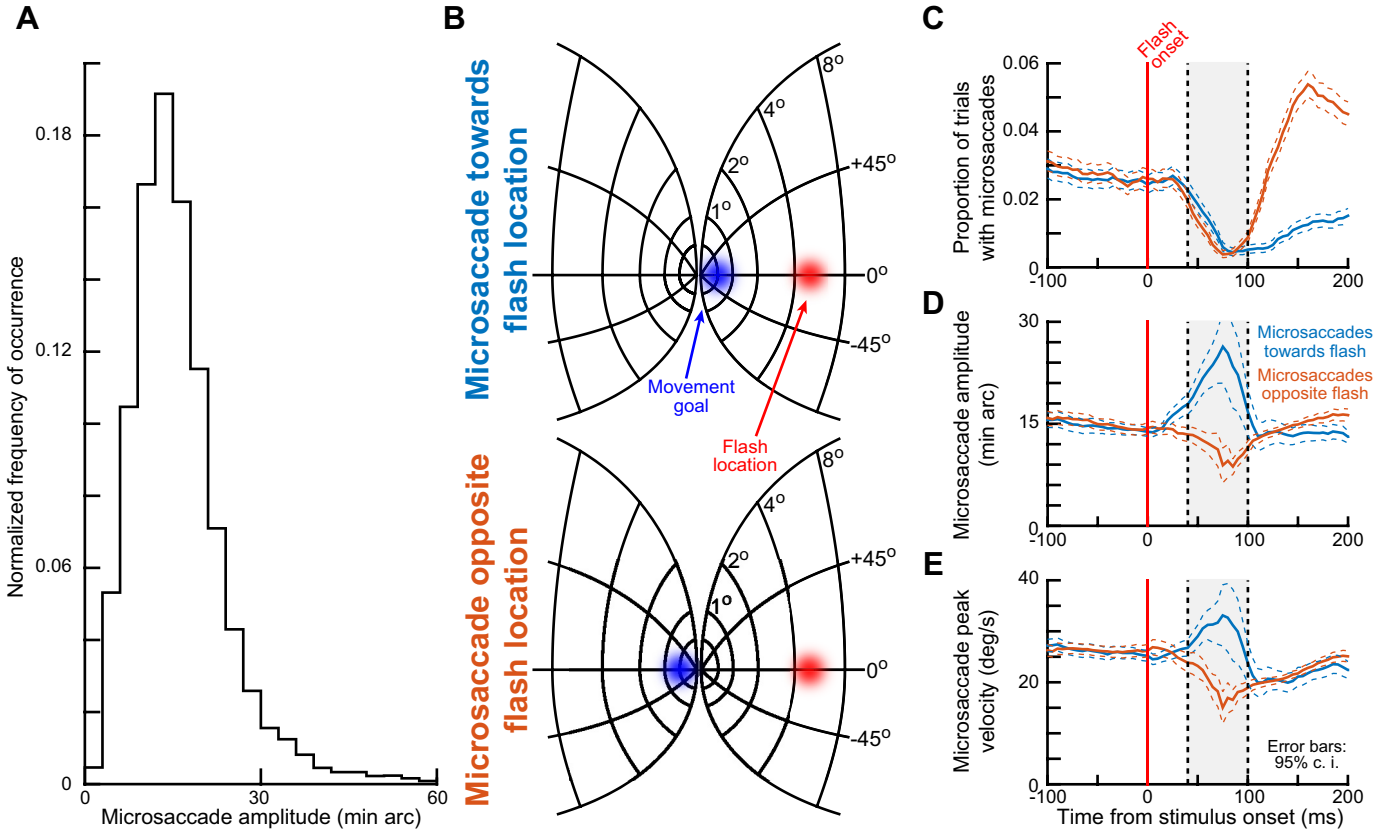

Fig. 2. Interactions between the spatial geometry of visual stimulus location and the saccade goal location in the phenomenon of kinematic alteration (*experiment 1*). *A*: in *experiment 1*, a microsaccade was planned to a near eccentricity, whereas a visual stimulus was presented peripherally. We confirmed this spatial dissociation by plotting the distribution of microsaccade amplitudes observed in the interval from −150 to 205 ms relative to peripheral stimulus onset. Median microsaccade amplitude was 13.18 min arc, more than an order of magnitude less eccentric than the peripheral stimulus location (MATERIALS AND METHODS). This is consistent with previous observations in monkeys and humans (Chen and Hafed 2013; Hafed et al. 2009; Hafed 2013). The histogram shown was normalized by the total number of observations (9,314 microsaccades from both monkeys). *B*: on a model of the SC map (Hafed and Chen 2016), the spatial dissociation is shown for a microsaccade either toward the flash location (*top*) or opposite it (*bottom*). In each case, the blue region of the spatial map would be the region of movement-related spiking activity at the time of movement execution, and the red region would be the region of stimulus-induced visual spikes that would occur after stimulus onset. Spatial readout of the map in the 2 scenarios predicts different patterns of executed saccade amplitudes. *C*: stimulus onset resulted in microsaccadic inhibition, as expected. graphs show the proportion of trials containing either "toward" (bluish color) or "opposite" (brownish color) microsaccades as a function of time after stimulus onset. Classic microsaccadic inhibition occurred. Note that the strong postinhibition difference between toward and opposite movements is expected given previous results (e.g., Tian et al. 2016). *D*: time courses of microsaccade radial amplitude as a function of time relative to peripheral stimulus onset. Near the time of microsaccadic inhibition (e.g., shaded region), microsaccade amplitude was modulated in a manner consistent with the predictions of spatial readout of oculomotor maps as in *B*. Toward microsaccades were consistently larger than opposite microsaccades. *E*: microsaccade peak velocity was also modulated, and one of our purposes in this study was to explore the relationships between the amplitude and peak velocity modulations (e.g., Figs. 4 and 7). Error bars denote 95% confidence intervals (c.i.).

period (e.g., during the time represented by the shaded region of Fig. 2, *C–E*). To demonstrate this, Fig. 3*A* shows three example pairs of microsaccades of different amplitudes from either *monkey N* (*left* pair) or *monkey P* (*middle* and *right* pairs). In each pair of microsaccades, the bluish curve describes the microsaccade that was directed toward the peripheral flash and the brownish curve describes the microsaccade that was directed opposite the peripheral flash. In all cases, the microsaccades were triggered during the time represented by the shaded region of Fig. 2, *C–E*. Importantly, in each pair, we selected microsaccades that were matched for peak velocity (compare the bluish and brownish eye velocity traces in the *bottom* row). As can be seen from the *top* row summarizing microsaccade radial amplitudes, even though the toward and opposite microsaccades had equal peak velocity in each pair, the toward microsaccades were consistently larger in radial amplitude (red arrows). Thus the toward and opposite microsaccades had different kinematics from each other, despite their minute sizes. Coupled with the data in Fig. 2, this suggests that the putative effects of spatial readout are not restricted to modulating amplitudes of saccades but that the modulation is also accompanied by alterations of movement kinematics, as well.

A complementary way to describe the phenomenon shown in Fig. 3*A* would be to pick example microsaccade pairs that were matched for radial amplitude instead of peak velocity, and to then check whether their peak velocities would be matched or not. If the microsaccades within a pair had similar kinematics, then the peak velocities should also be matched. However, they were not. In Fig. 3*B*, we picked three amplitude-matched pairs of microsaccades of different amplitudes (again, with the *left* pair from *monkey N* and the *middle* and *right* pairs from *monkey P*). In all pairs, the peak velocities of the opposite microsaccades were higher than those of the toward microsaccades. In other words, during microsaccadic inhibition, the original "planned" amplitudes of the opposite microsaccades might have been higher, but

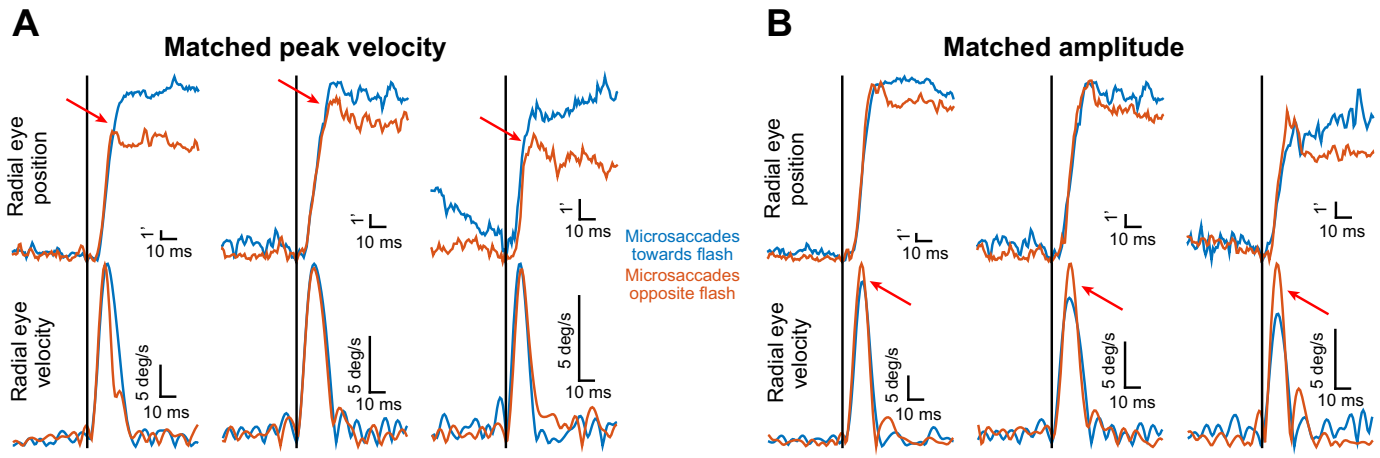

Fig. 3. Kinematic alteration of microsaccades occurring after peripheral stimulus onset. *A*: each column shows a pair of microsaccades that are matched for peak velocity. The pair at *left* is from *monkey N*, and the two pairs at *middle* and *right* are from *monkey P*. In the *top* row, radial eye position shows that the microsaccade toward the peripheral flash (bluish color) within a pair was larger than the microsaccade opposite the peripheral flash (brownish color) when these microsaccades were triggered during the microsaccadic inhibition period of Fig. 2*C*. This happened even though radial peak velocity was matched (*bottom* row). The 3 pairs were chosen to sample different microsaccade amplitudes (also see Fig. 8). *B*: a similar analysis to that in *A* but for pairs of movements that were matched for amplitude. In this case, even though the "toward" and "opposite" microsaccades within a pair were matched in radial amplitude, the peak velocity of the opposite microsaccade was larger, suggesting that a larger movement may have been planned, but there was spatial interaction like that shown in Fig. 2*B*, *bottom*, altering the executed microsaccade. Once again, the pair at *left* is from *monkey N*, and the two remaining pairs are from *monkey P*; also, the pairs were chosen to sample different amplitudes (also see Fig. 8). Figure 4 shows population summaries consistent with the example results presented in this figure, and the figure would be more suitable for inspecting velocity trajectories (beyond just peak velocity) more closely. This is because inspecting velocity trajectories for individual traces is less reliable given the low-velocity ripples associated with the differentiation operation needed to compute velocity (MATERIALS AND METHODS).

they were pulled down by the opposite visually induced spikes (Fig. 2*B*, *bottom*).

The results of Fig. 3 were obtained using example movements generalized across our data from *experiment 1*. In Fig. 4, *A* and *C*, we picked all microsaccades occurring 40–100 ms after flash onset and having a constant peak velocity (of 23°/s for *monkey P* and 25°/s for *monkey N*, based on each monkey's idiosyncratic range of microsaccade amplitudes). We then plotted radial eye position for toward and opposite microsaccades. Consistent with our hypothesis (Fig. 2*B*), toward microsaccades were consistently larger in each monkey than opposite microsaccades, despite the matched peak velocities ($P = 0.0265$ for *monkey P* and $P = 0.0015$ for *monkey N*, 2-tailed *t*-test). Interestingly, both monkeys also showed a small and short-lived dynamic reversal in microsaccade trajectory near movement end, but only for opposite microsaccades (Fig. 4, *A* and *C*); this rapid reversal was not present in the toward movements. Both of these observations suggest that readout of spatial maps may indeed play a role in movement kinematic alterations around the time of saccadic inhibition. Specifically, for the opposite movements, the antagonistic visual stimulus location may have served to dynamically reverse movement trajectory, resulting in the observed dynamic overshoot.

We then summarized all data during the inhibition period regardless of peak velocity (Fig. 4, *B* and *D*). For all microsaccades occurring 40–100 ms after peripheral flash onset, we plotted the ratio of peak velocity to movement amplitude separately for toward and opposite microsaccades. Because of the lawful main sequence relationship of saccades (Bahill et al. 1975; Zuber et al. 1965), this ratio is relatively constant across a large range of movement amplitudes, and a change in it between toward and opposite microsaccades would indicate different microsaccade kinematics between these two groups of movements. This was what we found for each of the monkeys; there was a statistically significant difference in kinematics between toward and opposite microsaccades, with toward microsaccades having higher amplitude and lower associated peak velocity (*P* values from 2-tailed *t*-tests are shown). Interestingly, we also calculated the ratio of peak velocity to amplitude during a baseline interval (−100 to −40 ms from stimulus onset) and plotted it as dashed gray lines in Fig. 4, *B* and *D*. As expected, the ratio during baseline was similar for toward and opposite microsaccades in each animal. However, in relation to the kinematic alterations after stimulus onset, the two animals showed opposite effects. Specifically, in *monkey P*, the kinematic alteration after stimulus onset primarily acted to increase the ratio in opposite movements; on the other hand, in *monkey N*, the kinematic alteration after stimulus onset primarily acted to decrease the ratio in toward movements. This might reflect differential weighting of spatial readout mechanisms in the two animals, as well as the possibility of temporal fluctuations in saccade kinematics in general and before stimulus onset (see DISCUSSION).

Our results so far demonstrate that even on the scale of microsaccades, visual transients are associated with kinematic changes of saccades, and that the amplitude changes observed are correlated with what is expected out of readout of spatial maps, like those in the SC. Moreover, the amplitude changes could be both increases or decreases depending on relative spatial layouts of flash and movement goal locations.

Kinematic Alterations in Microsaccades When the Flash and Movement Goal Are Virtually Colocalized

Studies of saccadic inhibition often use large flashes (e.g., full-screen flashes) or flashes remote from the saccade goal (e.g., Fig. 1*A*) to trigger inhibition (Bompas and Sumner 2011; Buonocore and McIntosh 2012; Buonocore et al. 2016; Edelman and Xu 2009; Guillaume 2012; Reingold and Stampe

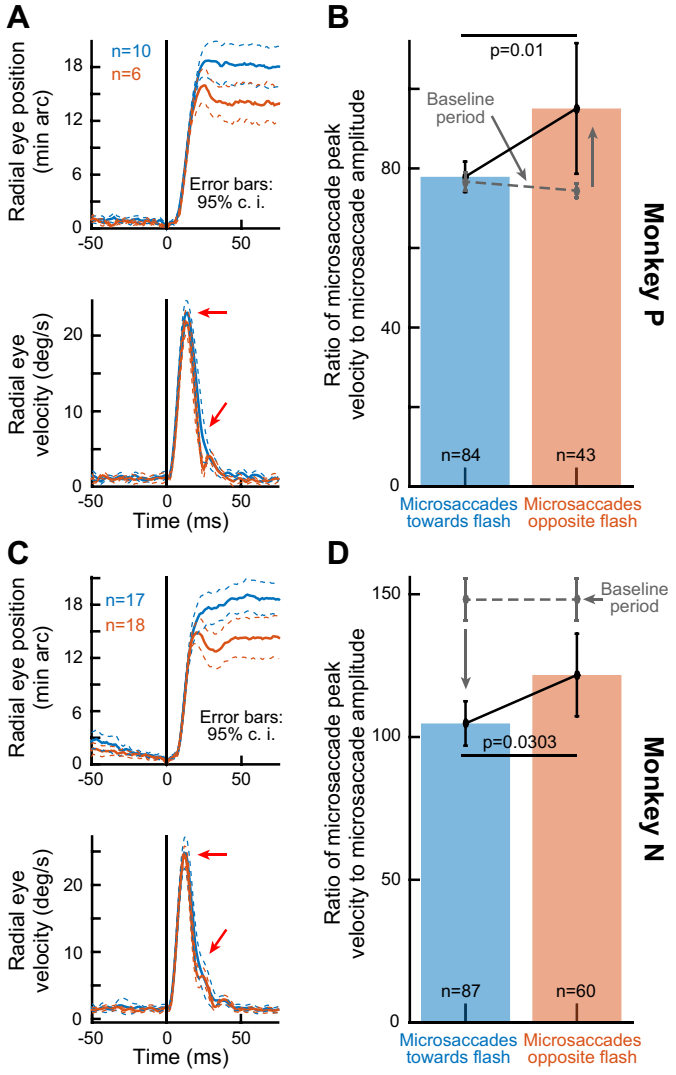

Fig. 4. Consistency of kinematic alterations of microsaccades between "toward" and "opposite" movements occurring near the time of microsaccadic inhibition. *A* and *C*: for each monkey, we selected all microsaccades occurring within 40–100 ms after peripheral stimulus onset (Fig. 2*B*) that had a certain peak velocity (see the eye velocity trace in each panel and the horizontal red arrow). For those microsaccades, we plotted the average radial eye position trace. Toward microsaccades were consistently bigger than opposite movements despite matched peak velocities. Note that the velocity traces suggest faster deceleration for the opposite movements (diagonal red arrows), which contributes to the reduced amplitudes (as is the case with large saccades; e.g., Figs. 1 and 10). *B* and *D*: for all microsaccades occurring 40–100 ms after stimulus onset (regardless of peak velocity), we plotted the ratio of peak velocity to movement amplitude. This ratio was different between toward and opposite microsaccades in each monkey. Thus, in addition to amplitude and velocity variations (Fig. 2, *D* and *E*), the kinematics of microsaccades were also altered by the recently appearing visual flash. The gray data show the same ratio but for microsaccades occurring from −100 to −40 ms from stimulus onset. Error bars in all panels denote 95% confidence intervals.

2000, 2002). However, it is still not entirely clear how close the flash can be to the saccade goal location and still result in either inhibition or kinematic alterations. We explored this issue using microsaccades; because these movements correct minute foveal errors during fixation (Guerrasio et al. 2010; Ko et al. 2010; Tian et al. 2016), there is a high likelihood that any given microsaccade is goal directed and reduces a foveal motor error away from the fixation spot. If so, then introducing a visual flash directly at the fixation spot makes the flash location and the saccade goal location very close to each other, as shown in Fig. 5*A*, with typical dimensions of our microsaccades and with the size of our fixation spot.

We repeated *experiment 1* (Fig. 2), this time introducing a visual transient on the fixation spot itself (*experiment 2*). The transient was a brief dimming of the spot to black and then back to white (MATERIALS AND METHODS). We classified microsaccades in this experiment as being either toward or opposite the flash location (*insets* in Fig. 5*C*), which renders the current experiment conceptually identical to that in Fig. 2*B*, except that the flash location was much closer to the movement goal, particularly for the toward microsaccades (Fig. 5*A*). We first confirmed that during maintained fixation, toward microsaccades reduced foveal motor error, whereas opposite microsaccades increased it (Fig. 5*B*). In other words, for toward microsaccades, the end points of the movements were closer to the fixation spot than the end points of opposite microsaccades (Fig. 5*C*). Thus our intuition that this experiment would be conceptually similar to *experiment 1* is reasonable.

Despite the proximity of the flash to the saccade goal, microsaccade rate still showed robust inhibition after flash onset in this experiment. Figure 6*A* shows the proportion of microsaccades occurring near the time of foveal flash onset for toward and opposite microsaccades relative to the fixation spot location. As can be seen, robust microsaccadic inhibition occurred regardless of movement direction. This is interesting because flash and goal location were very close, especially in the toward microsaccades in this experiment, unlike in *experiment 1* (Figs. 2–4). Importantly, note that the great majority of microsaccades were toward movements (also see the *z*-axis color scales in Fig. 5*B*). This confirms prior results (Tian et al. 2016) demonstrating that microsaccades in experiments with sensory transients primarily occur to correct and optimize eye position relative to the fixated foveal stimulus. Moreover, the microsaccade amplitudes themselves were small (Fig. 6*B*), suggesting that the interaction between movement goal and stimulus location was occurring well within the foveal representation.

Thus this experiment has revealed that robust inhibition still occurs even when the flash location is very close to the movement goal location, consistent with experiments in humans (Buonocore and McIntosh 2012). We next turned to exploring microsaccade metrics and kinematics. In terms of metrics, microsaccade amplitudes also showed very similar patterns to those in *experiment 1* with the peripheral stimulus onset. That is, for microsaccades toward the fixation spot, the flash of the fixation spot resulted in larger movement amplitudes in each of the monkeys (Fig. 7*A*, second row). For the very few microsaccades that were opposite the fixation spot, their amplitude was not increased (although the rarity of these movements makes it hard to assess statistical reliability of this observation, and we do not show the data in Fig. 7*A* to avoid clutter). These results are all very similar to those observed in Fig. 2, *C* and *D*, and they suggest that the end points of individual microsaccades are under exquisite control by the oculomotor system, even with minute foveal differences between eye and target location. Consistent with this, we found that the microsaccades affected by the foveal flash in the present experiment landed more accurately near the center of the fixation spot compared with earlier microsaccades (Fig.

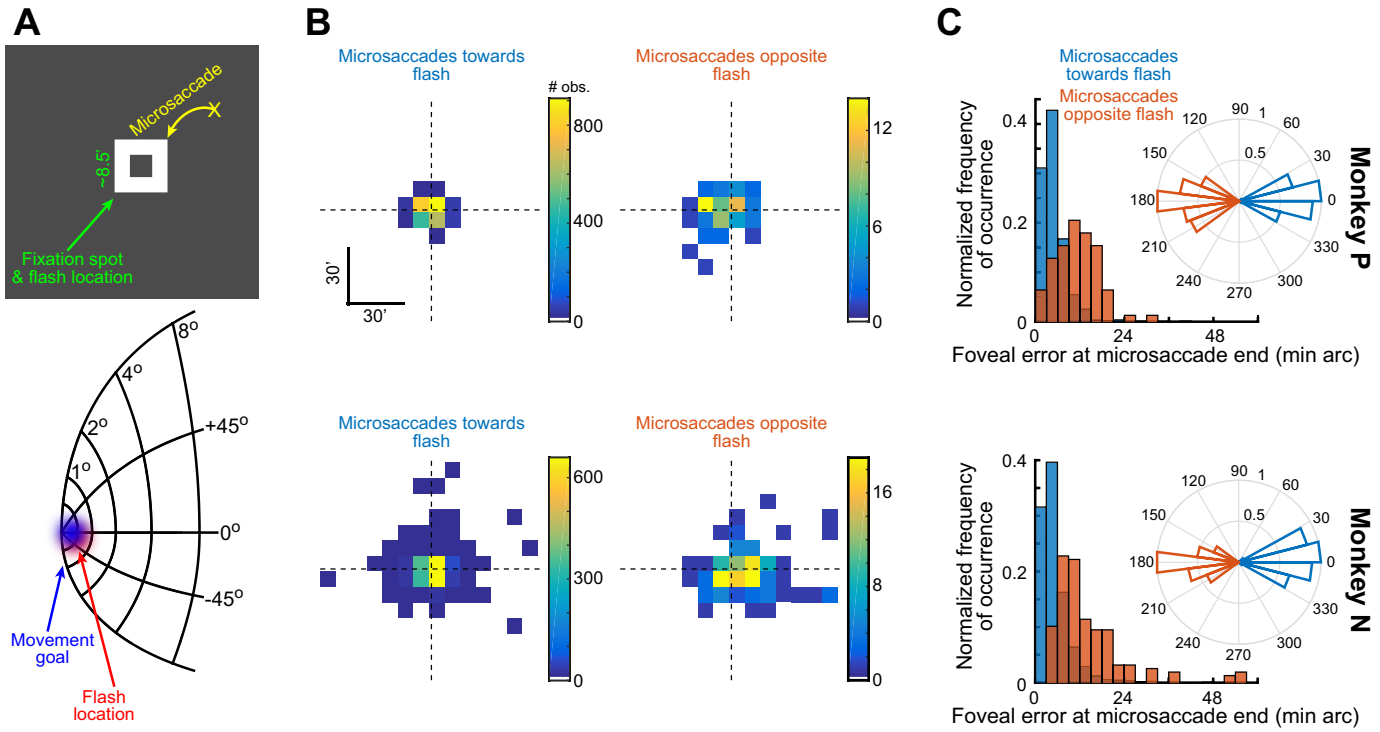

Fig. 5. Exploring microsaccadic inhibition and kinematic alterations when the flash and movement goal are almost colocalized (*experiment 2*). *A*: the logic of *experiment 2*. If a microsaccade is triggered to correct for a foveal motor error, then the fixation spot (a white "frame" of pixels with a hole in the middle) is close to the movement goal of the microsaccade (*top*). Thus introducing a transient flash on the fixation spot makes the flash-related and movement-related spikes in oculomotor maps like the SC map model shown (Hafed and Chen 2016) almost colocalized. *B*: in each monkey (i.e., within each row), we plotted the distribution of landing eye positions at microsaccade end for either "toward" (*left* plot) or "opposite" (*right* plot) microsaccades. Toward and opposite movements were classified according to the *inset* polar plots in *C*, showing microsaccade angle relative to the axis connecting eye position at movement onset and the center of the fixation spot (Materials And Methods). Toward microsaccades brought gaze closer to the fixation spot (also shown in more detail in *C*). Moreover, there were many more toward than opposite microsaccades. *C*: for either toward or opposite microsaccades, and for each monkey individually, we plotted a normalized histogram of the final eye position after microsaccade end (i.e., the final foveal motor error). Toward microsaccades consistently decreased eye position error (compare bluish and brownish histograms in each monkey; $P < 0.00001$ for each monkey, Wilcoxon rank sum test). Note that the histograms were normalized to facilitate viewing of the different landing eye position errors. In reality, there were very few opposite microsaccades (see *B* and Fig. 6*A*).

7*B*). Specifically, we plotted the remaining foveal error at microsaccade end (similar to the analysis shown in Fig. 5) for either microsaccades after foveal flash occurrence or microsaccades before it. The post-flash microsaccades had a median landing error of 3.6 and 3.9 min arc in *monkeys P* and *N*, respectively, compared with a median of 4.4 and 4.2 min arc for *monkeys P* and *N* in the pre-flash microsaccades ($P < 2.9120e\text{-}13$ and $P < 0.002$ for *monkeys P* and *N*, respectively). Although this effect is expectedly small in amplitude given the small sizes of microsaccades and foveal errors involved during

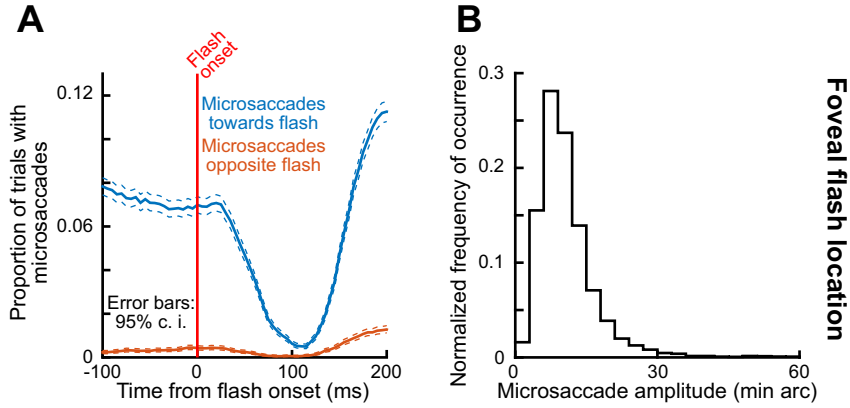

Fig. 6. Microsaccadic inhibition occurs even when flash and movement goal location are almost colocalized and foveal. *A*: we plotted the proportion of trials containing microsaccades as a function of time from foveal flash onset. Regardless of microsaccade direction relative to the flash location (either bluish or brownish curve), robust microsaccadic inhibition occurred. This was particularly true for toward movements (bluish curve) even though the flash was almost perfectly colocalized with the movement goal (Fig. 5*A*). Also, note that the frequency of opposite microsaccades is much less than that of toward movements (compare bluish and brownish curves). This is consistent with observations that microsaccades occur to primarily correct instantaneous foveal motor error (Tian et al. 2016). Error bars denote 95% confidence intervals. *B*: microsaccade amplitude distribution in the present experiment (similar to how it was computed in Fig. 2*A*), demonstrating the small scale of movement goal and stimulus locations that we tested in this portion of our study.

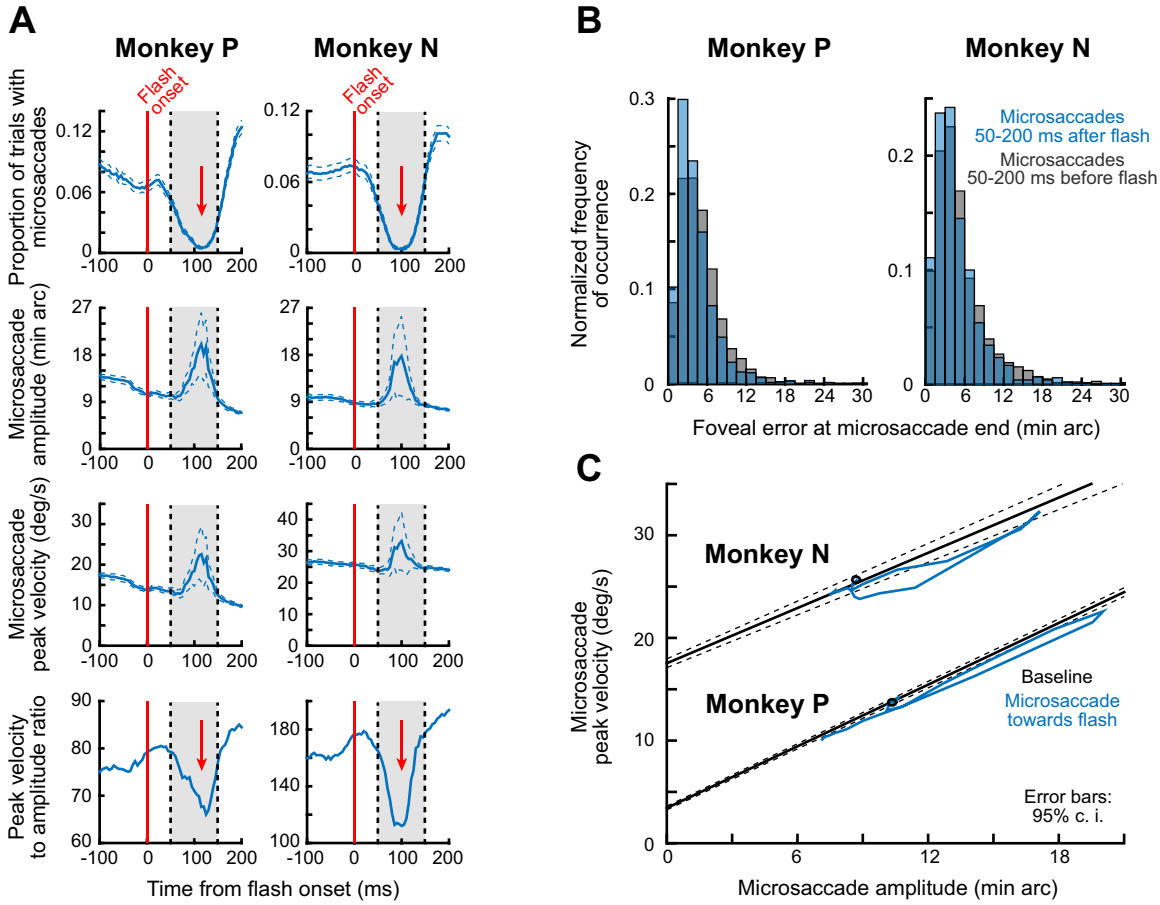

Fig. 7. Microsaccade kinematic alteration with a foveal flash. *A*: for "toward" microsaccades (Figs. 5 and 6), we plotted time courses of rate (*top* row), amplitude (second row), peak velocity (third row), and ratio of peak velocity to amplitude (*bottom* row). In each monkey, microsaccadic inhibition occurred despite the proximity of movement goal and flash location (*top* row). Around the inhibition period, movement amplitude (second row) and peak velocity (third row) increased, consistent with spatial readout predictions (Figs. 2–4 and 5*A*). Moreover, the peak velocity increase was not proportional with the amplitude increase, resulting in a transient dip in ratio of peak velocity to movement amplitude (*bottom* row). This suggests an alteration in microsaccade kinematics. *B*: the alterations observed in *A* resulted in post-flash microsaccades that landed more accurately at the goal location than those without the flash, consistent with the hypothesis that spatial readout "pulls" the microsaccades toward the flash location. For each monkey, we plotted the foveal error at microsaccade end (i.e., the remaining distance to the fixation point center after microsaccade end) for movements occurring either shortly after the flash (bluish) or before the flash (gray). There was a small but systematic reduction in foveal error in each animal for movements occurring right after the flash (median error with the flash was 3.9 and 3.6 min arc in *monkeys N* and *P*, respectively, whereas it was 4.2 and 4.4 min arc before the flash; $P < 0.002$ for each monkey). This suggests that the flash had a functional impact of increasing microsaccade landing accuracy. *C*: microsaccade kinematic alterations can also be seen when peak velocity is plotted against amplitude (i.e., the main sequence curve). For baseline microsaccades (−150 to 0 ms from flash onset), we fitted the main sequence curve and obtained 95% confidence intervals (MATERIALS AND METHODS). For toward movements occurring 5–205 ms after flash onset, we then plotted the trajectory of peak velocity and amplitude from the curves in *A* (in steps of 10 ms). The black circle indicates time 5 ms, and the phase plane curves show progress from 5 ms onward. Microsaccades were consistently deviated from the baseline curve. Note that the monkey had different peak velocities (compare black curves), and this was due to different amounts of microsaccade curvature between the animals. Error bars in all panels show 95% confidence intervals.

accurate fixation by our monkeys (Tian et al. 2016), it does indicate that the flash served to "pull" the microsaccade end points even more accurately toward it, as per our hypothesized mechanism of Fig. 1.

The similarity of the amplitude effects in the present experiment with those in *experiment 1* (Figs. 2–4) also extended to microsaccade kinematic alterations. Specifically, the third row of Fig. 7*A* shows the time course of microsaccade peak velocity around the time of the microsaccadic inhibition period. For the microsaccades directed toward the foveal flash, peak velocity increased like amplitude did. However, the increase was not proportional such that there were kinematic alterations: the fourth row shows a transient decrease in the ratio of microsaccadic peak velocity to microsaccadic amplitude, similar to that observed in Fig. 4. Therefore, even with foveal flashes, microsaccadic kinematic alterations occur in association with microsaccadic inhibition.

We also explicitly compared main sequence curves in each of the monkeys during this task. In Fig. 7*C*, we plotted peak velocity vs. amplitude for microsaccades that we detected in the present experiment. For each monkey, the black curve describes the main sequence curve obtained in baseline (0–150 ms before flash onset) from a large number of movements during steady fixation and before flash onset (>3,300 in each monkey). We fitted the measurements from this large number of movements using linear regression, and Fig. 7*C* (black) shows the mean and 95% confidence intervals of these fits. Note that each monkey had a slightly different observed peak velocity for a given amplitude from the other monkey, and this is likely due to different amounts of microsaccadic curvature in

the two animals. In any case, we then took the time courses of amplitude and peak velocity in the second and third rows of Fig. 7*A* for each monkey, and we plotted these time courses (from 5 to 205 ms after flash onset) as a trajectory in peak velocity-vs.-amplitude space. This resulted in the bluish phase-plane curves in Fig. 7*C*, which were below the baseline main sequence curve in each animal. Therefore, each animal showed a consistent violation of its baseline microsaccade kinematic characteristics, as shown in Fig. 7*A* and also as shown in *experiment 1* (Figs. 2–4).

The kinematic variations of microsaccades that we observed in this experiment also occurred for even the smallest movement amplitudes that we could detect. Specifically, we summarized the alteration in microsaccadic kinematics in each monkey for different movement amplitudes and different times after flash onset. In Fig. 8, the *x*-axis in each panel describes a microsaccade amplitude bin, and the *y*-axis describes a "violation index" based on that in Buonocore et al. (2016). This index is 1 if the peak velocity and amplitude relationship is similar to the animal's baseline, and it is different from 1 if there are microsaccadic kinematic alterations during the analyzed interval of each panel. In black, we plot the index for baseline microsaccades obtained from a 150-ms interval before flash onset; such index was expectedly close to 1. On the other hand, in the bluish curves, we show the index for toward microsaccades occurring within different 50-ms intervals after flash onset (each panel is a different 50-ms interval as shown in the *insets*). As can be seen, in both monkeys, all microsaccade amplitude bins showed violation of the main sequence relationship between peak velocity and movement amplitude for the time intervals in which microsaccadic inhibition occurred (compare 95% confidence intervals between black and bluish curves for the 50-ms intervals near microsaccadic inhibition). Therefore, kinematic alterations can happen even for the smallest possible saccades. The duration of such kinematic alteration was slightly different between the two animals, but so was the duration of the inhibition phenomenon, as well.

Taken together, our results so far demonstrate that kinematic alterations after visual transients occur even for microsaccades, and regardless of whether the visual transient is peripheral or foveal.

Generalizability of Monkey Kinematic Alterations to Larger Saccades

Finally, in *experiment 3*, we explored whether monkeys can replicate previously reported human results with large saccades (Buonocore et al. 2016), so we trained one monkey (*monkey N*) to freely view a cloud pattern like that shown in Fig. 9. In this figure, an example eye movement scan path is also shown in cyan color. At a random time during such free viewing (MATERIALS AND METHODS), the whole display underwent a transient flash of ~16 ms in duration (to either black or white). If the monkey happened to generate a saccade toward one corner of the display after flash onset (as per the spatial constraints detailed in Fig. 9*B*), then this situation is akin to a

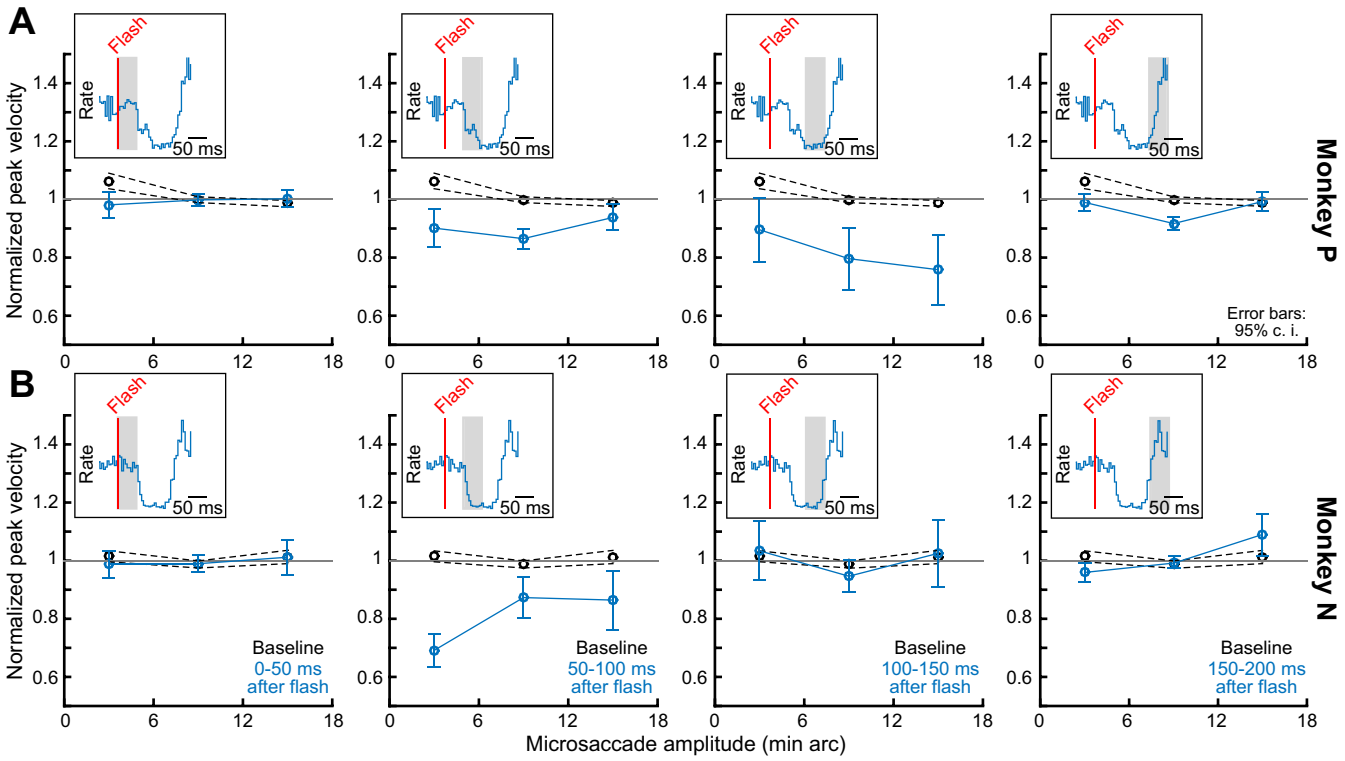

Fig. 8. Alteration of microsaccade kinematics regardless of microsaccade amplitude. In each monkey (*A* and *B*), we plotted an index of kinematic alteration (MATERIALS AND METHODS) similar to the one used in Buonocore et al. (2016), and we plotted it for different microsaccade amplitude bins (*x*-axis in each graph; bin width = ±3 min arc around each shown bin center). Each graph shows a different time period relative to flash onset. For microsaccades very close (leftmost column) or very far (rightmost column) from the time of flash onset, no strong kinematic alteration occurred. However, near the microsaccadic inhibition period (i.e., when visual spikes are expected to interact with movement-related spikes in Fig. 1), kinematic alteration like that in Fig. 7 was observed, and this happened for all microsaccade amplitude bins. Thus kinematic alteration occurs even for the smallest possible saccades. Note that the effect was longer lived in *monkey P* than in *monkey N*, but so was this monkey's inhibition period, as well (see *insets*). Error bars denote 95% confidence intervals.

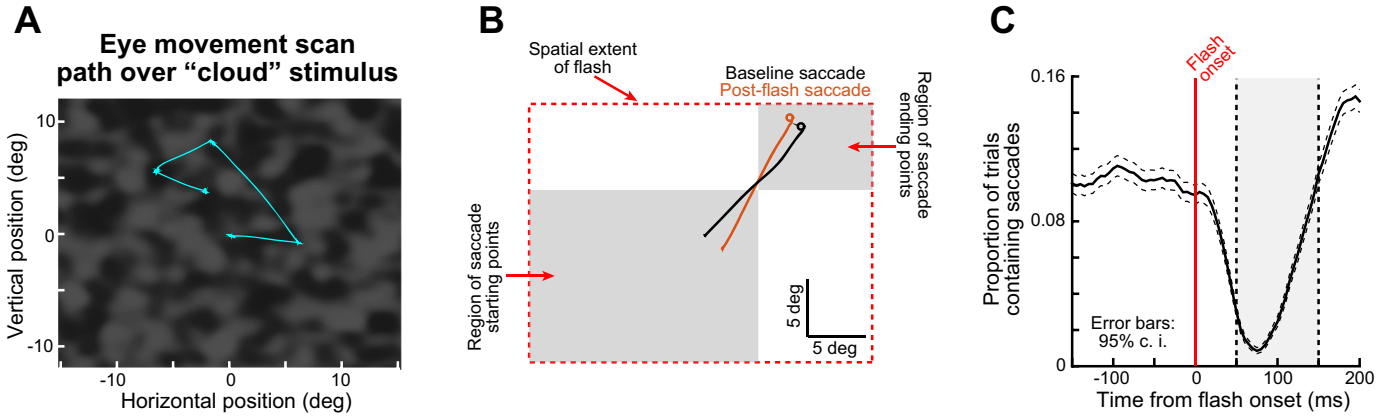

Fig. 9. Free-viewing task of *experiment 3* and its analysis. *A*: the monkey scanned a cloud pattern, and a transient full-screen flash occurred at a random time. Example eye movement scan paths are shown in cyan. *B*: we selected either baseline saccades occurring 20–200 ms before flash onset (black example saccade) or post-flash saccades occurring 50–150 ms after flash onset (brownish example saccade). Saccades were chosen such that, relative to the flash geometry (i.e., the screen extent), their starting and ending eye positions fell within the gray regions shown. Specifically, we split the screen into 9 equally sized virtual tiles; any saccade starting from a large region of 4 contiguous tiles abutting one corner of the display (e.g., the large gray box) and ending into a single tile in the opposite corner (e.g., the small gray box) was considered as a saccade for which the flash (i.e., the full-screen stimulus) had a center of mass less eccentric than the saccade goal location (similar to opposite movements in our earlier analyses with microsaccades). Note that we repeated this tiling procedure for all other corners of the screen. Thus, with such selection, we ensured that the center of mass of visual spikes associated with the full-screen flash was less eccentric than the center of mass of the saccade goal location (as in the schematic scenario of Fig. 1*C*), which would allow replication of previous human experiments (it is also conceptually similar to opposite microsaccades in Fig. 2). *C*: we confirmed that for these saccades, saccadic inhibition occurred in the monkey (e.g., gray region), as with earlier human experiments and our earlier microsaccade experiments. Error bars denote 95% confidence intervals.

flash having a center of mass less eccentric than the saccade goal location in retinotopic coordinates. Thus this scenario could allow us to replicate previous human experiments in our monkey. To do this systematically, we designated regions of the display as starting or ending regions, and we selected saccades consistent with these regions. For example, in Fig. 9*B*, the saccade had to originate from the *bottom left* region of the display and end in the *top right* region. We also had similar regions for all four corners of the display such that the ending region was always near a corner and the starting region was nearer to the opposite corner (i.e., with primarily diagonal saccades). We then selected either baseline saccades (black in Fig. 9*B*) or saccades occurring during saccadic inhibition (50–150 ms after flash onset; brownish saccade in Fig. 9*B*). As expected, the flash caused robust saccadic inhibition in this task (Fig. 9*C*), which allowed us to look for saccade kinematic alterations. Of course, smaller flashes might have given rise to larger effects on these kinematics, perhaps due to computational considerations of lateral inhibition (Mégardon et al. 2015), but the robustness of the inhibition that we saw in Fig. 9*C* suggests that we were still in a good position to analyze kinematic alterations.

For the matched saccade vectors between baseline and inhibition phases according to the selection criteria of Fig. 9*B*, we plotted the main sequence curve for baseline saccades (occurring 20–200 ms before flash onset). This is shown as the black curve in Fig. 10, *A* and *B*. For each saccade amplitude bin (2.17° wide), we plotted the mean and 95% confidence interval for peak velocity at this bin. We then selected matched saccades in terms of starting and ending regions (as in Fig. 9*B*), but they occurred either 0–50 ms after flash onset (Fig. 10*A*, brownish curve) or 50–150 ms after flash onset (Fig. 10*B*, brownish curve). As can be seen, for Fig. 10*A*, the main sequence curve was not altered by much because the saccades were occurring too soon after flash onset and before saccadic inhibition. However, during the saccadic inhibition period (Fig. 10*B*), the main sequence curve showed higher peak velocities than expected (compare brownish and black curves), and this was particularly strong for large saccades. For example, for saccades of ~13° amplitude (Fig. 10*C*), peak velocity during saccadic inhibition was 12% higher than during baseline, even when saccade amplitude was fixed. Other saccade amplitude bins are also shown in Fig. 10*D* for completeness. These results demonstrate that our microsaccade results from *experiments 1* and *2* (Figs. 2–8) generalize to larger saccades.

DISCUSSION

We found that microsaccade kinematics can be altered by recently appearing peripheral or foveal visual stimuli. Our behavioral results suggest that spatial readout of oculomotor maps during saccade execution may be affected by the presence of coincident "visual spikes." In what follows, we discuss how these results inform mechanisms of microsaccade and saccade generation, as well as broader mechanisms of saccadic inhibition.

A Putative Mechanism for Saccadic Inhibition and Kinematic Alteration

Models of saccadic inhibition often invoke the SC (Bompas and Sumner 2011). When a flash occurs, it interacts with ongoing presaccadic activity, resulting in saccadic inhibition. Such interaction has been observed neurophysiologically (Dorris et al. 2007): neurons encoding the saccade target experience a transient activity dip when a remote distractor is flashed and a saccade is successfully delayed.

We believe that SC involvement in saccadic inhibition also critically depends on neurons responding to the flash and not just the saccade goal, and that its involvement is part of a fine orchestration with other brain stem structures. Specifically, visual input associated with the flash affects both the SC and premotor neurons, including OPNs (Fig. 11). We think that

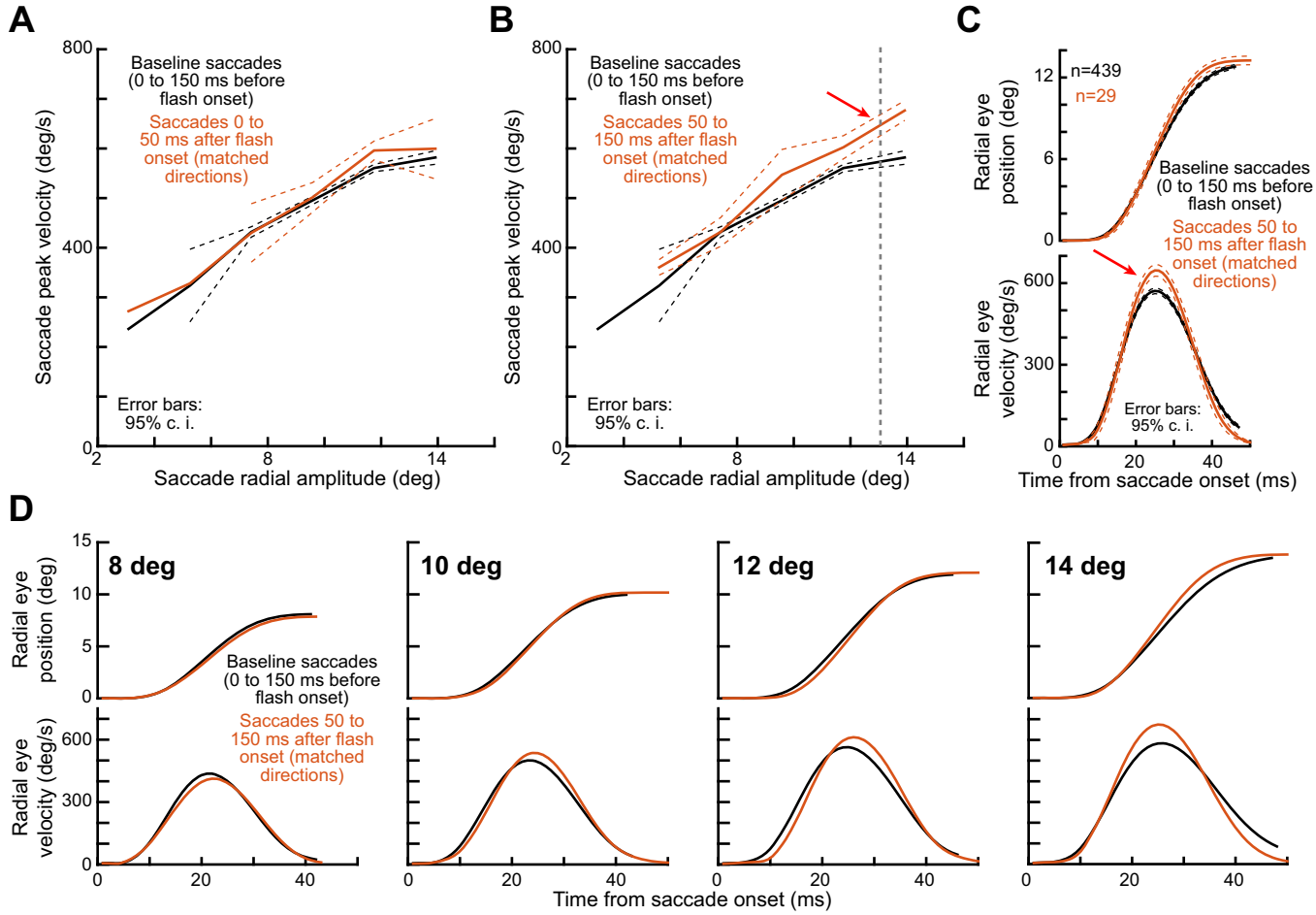

Fig. 10. Kinematic alteration for large monkey saccades. *A*: we plotted the main sequence curve for baseline saccades (black) or post-flash saccades (brownish) after saccades were selected according to the criteria of Fig. 9*B*. The main sequence curves were close to each other, because the flash was too close in time to the saccade onset (visual spikes would arrive too late after the saccade has been triggered to influence it). *B*: however, for saccades occurring near saccadic inhibition time (i.e., when visual spikes would coincide with saccade triggering), the main sequence curve was consistently elevated, especially for larger saccades. This is consistent with results of previous human experiments (Buonocore et al. 2016) and also with our microsaccade results from earlier figures (for opposite microsaccades). *C*: for an example saccade amplitude bin from *B* (all saccades with amplitude 13.5 ± 1.5°), we could confirm that peak velocity was consistently elevated for the same movement amplitude. *D*: we repeated the analysis shown in *C* but for other saccade amplitude bins centered on 8°, 10°, 12°, and 14°. Each bin included saccades ±0.5° in amplitude relative to the bin center. As expected from data in *B*, peak velocity alterations were consistent for all the different saccade amplitudes, except for 8° saccades (this is likely due to the small saccade size relative to the flash center of mass). Error bars denote 95% confidence intervals.

visual input arrives at both a "Go" system, including spatial maps that define movement metrics, as well as a "Pause" system that helps control saccade timing, as in OPNs (Fig. 11*A*). The arrival time of visual spikes at both the Go and Pause systems dictates the probability of saccade generation. For example, in the scenario in Fig. 11*B*, *left*, visual spikes after flash onset arrive not only at the Go system but also at the Pause system, and they do so early enough before the pause is executed. This may be sufficient to prevent saccades from reaching execution threshold (Hafed and Ignashchenkova 2013), and saccades would therefore be delayed. Neurophysiologically, it was indeed found that some OPNs exhibit a short-latency transient activity increase after visual onsets (Everling et al. 1998; Missal and Keller 2002), and we think that this can delay saccades. On the other hand, in the scenario in Fig. 11*B*, *right*, the Pause system might already be turned off despite the visual input (perhaps because the visual spikes arrive too late to prevent OPNs from pausing). In this case, a saccade will be triggered nonetheless, exactly when the Go system has not only saccade-related spikes describing the saccade goal location but also additional visual spikes (Fig. 1). Thus kinematic alterations might arise because of fine timing relationships between the arrival of visual flash-related spikes and the gating of eye movements by the Pause system.

It is interesting to note that our hypothesized mechanism is consistent with experimental manipulations that have inserted "artificial" spikes into either the Pause or Go signal. For example, McPeek et al. (2003) used subthreshold electrical stimulation of the SC at a locus different from the saccade goal location, and they were able to cause strong deviations in saccade trajectories when stimulation was applied during an appropriate time window just before movement onset. Conversely, blink perturbations have been used to inhibit OPNs (i.e., disinhibit the saccadic system) to fine-tune models of saccade control (Katnani and Gandhi 2013; Katnani et al. 2012b; Rottach et al. 1998; Schultz et al. 2010). In this regard, it is also expected that other sensory modalities can elicit saccadic inhibition, since they can also introduce stimulus-

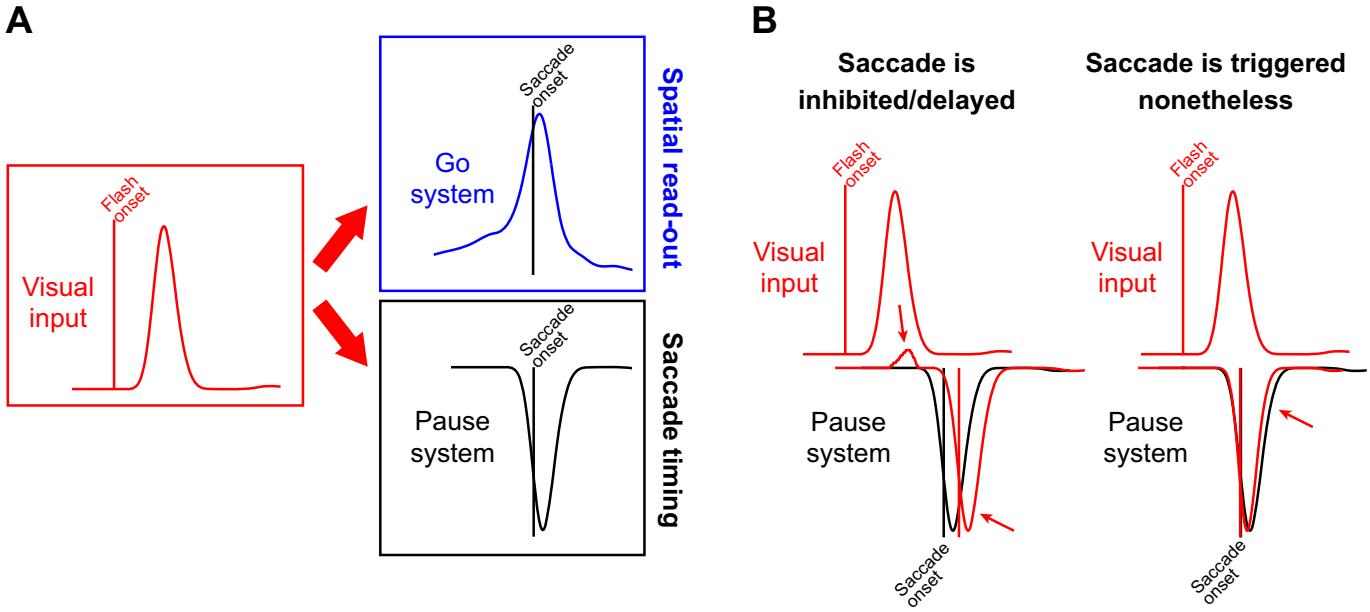

Fig. 11. Hypothesized mechanism for saccadic inhibition and kinematic alterations. *A*: visual transients result in visual input to a variety of oculomotor structures (red). Among these structures are spatial ones (e.g., the SC) in which spatial readout of activity would be altered by the visual spikes present at movement triggering (blue "Go" system). Additionally, other structures (e.g., omnipause neurons, OPNs) are part of a "Pause" system (black) that helps gate saccades and influence saccade timing. If the Pause system happens to be already in the "off" state at the time of presence of visual spikes in the Go system (e.g., Fig. 1*C*; i.e., the saccade is being executed), then spatial readout of the Go system would alter movement kinematics. *B*: saccadic inhibition may be a result of the timing of visual inputs arriving to the Pause and Go systems. In the scenario at *left*, the visual stimulus appears early enough before pause onset such that visual input to the Pause system delays any potential eye movement triggering (red arrows). In this case, saccades are delayed, explaining the classic saccadic inhibition "dip" in reaction time distributions. In the scenario at *right*, the saccade is triggered nonetheless such that at the time of pause in the Pause system (i.e., at the time of saccade execution), visual spikes are present anyway in the Go system and can alter saccade kinematics. Note that the visual spikes may also contribute to reactivating the Pause system a bit early (red arrow) and truncating saccades. Therefore, saccade amplitudes and peak velocities can still be altered by the visual input, even if some truncation may still occur in the same movements.

related "spikes" in either the Go or Pause systems, or both. For example, some authors were able to observe robust saccadic or microsaccadic inhibition with auditory stimulation (Graupner et al. 2007; Pannasch et al. 2001; Rolfs et al. 2008), although for large saccades, other authors could not replicate these findings (Reingold and Stampe 2004).

In any case, one advantage of our hypothesized mechanism is that it provides neurophysiologically testable hypotheses about both saccadic inhibition and kinematic alterations. So far, the mechanisms for the latter are not well understood. In the three key studies that have explored this phenomenon in humans (Buonocore et al. 2016; Edelman and Xu 2009; Guillaume 2012), a common finding was that saccades near the inhibition period had reduced amplitude but higher peak velocity. This may be reminiscent of saccade interruption (Keller and Edelman 1994). However, saccade amplitude increases (relative to peak velocity) can also occur (e.g., Fig. 8), suggesting that in the scenario in Fig. 11*B*, *right*, spatial readout in the Go system might play a role. Of course, the Pause system might still get reactivated earlier than baseline because of the visual input (rightmost red arrow in Fig. 11*B*). In this case, both spatial readout and saccade truncation can co-occur, but we do not yet know whether visual input can reactivate paused OPNs. Certainly, comparison of the baseline data in Fig. 4, *B* and *D*, with the data after stimulus onset suggests that interruption can indeed be a strong factor, at least in some individuals like *monkey P*. In any case, future studies of brain stem premotor nuclei will need to clarify these hypotheses, as well as inform detailed timing differences that may appear between our monkey studies and earlier human experiments (showing slightly earlier effects). In particular, because very little is known about the properties of visual responses of OPNs, investigating these responses and their relation to visual responses in the SC, as well as investigating how/whether they might interfere with saccade generation, can provide a lot of insights. Additionally, analysis of microsaccadic inhibition during SC inactivation (Hafed et al. 2013) but from the perspective of kinematic alterations would also be interesting, especially in combination with attempts to explore the mechanisms behind potential differences in inhibition profiles between flash locations in either the same or opposite hemifield from a given microsaccade (e.g., Fig. 2*C*).

Another advantage of our hypothesized mechanism is that it can deal with the microscopic scale of microsaccades relatively easily, even though computationally, microsaccades would cause activation near the edge of a simulated map (and therefore suffer from computational "edge effects"). Specifically, we found a precise influence of saccadic inhibition even when the flash and the movement goal are virtually colocalized (Fig. 5). Given the coarse population coding schemes of structures such as SC (see below), models that show saccadic inhibition (e.g., Bompas and Sumner 2011) are most successful when flash and movement goal are spatially highly segregated and far from map edges. In fact, with near distractors, SC activity shows correlates of "capture" instead of "inhibition" (Dorris et al. 2007). On the other hand, if the phenomenon of saccadic inhibition is a function of precise timing between visual input and the activity of the Pause system (Fig. 11), then it is easier to explain our results with a foveal flash (e.g., Figs. 5–8), as well as related human results with large saccades (Buonocore

and McIntosh 2012). This is so because timing in our mechanism is somewhat independent of spatial representation, similar to earlier proposals (Findlay and Walker 1999). In the future, it would also be interesting to explore the role of the cerebellum (Arnstein et al. 2015) in kinematic alterations, and also to relate our hypothesized mechanism with other saccade phenomena, such as the "global effect" (Findlay 1982; Walker et al. 1997).

Finally, our hypothesized mechanism is not inconsistent with the idea that saccade triggering may be an emergent property of recurrent loops in midbrain and brain stem oculomotor nuclei. Specifically, it is known that the SC projects to OPNs (Büttner-Ennever et al. 1999; Gandhi and Keller 1997) as well as to premotor burst neurons (Strassman et al. 1987), and that premotor nuclei also project back to the SC (Arai et al. 1999; Hartwich-Young et al. 1990). Thus the trigger for a saccade occurs when the network components of the Go and Pause systems evolve into a specific neural state where premotor burst neurons emit a burst and OPNs exhibit a pause; our model is agnostic of the specific implementation of this trigger as long as visual inputs can alter both the Go and Pause components.

Potential Role of the SC in Dictating Saccade Metrics

Our observation of spatial interactions between visual flash geometry and the movement end point is interesting in light of recent SC saccade control models (Goossens and Van Opstal 2010, 2012; Katnani et al. 2012). These models posit that during the SC "saccade burst," each spike contributes a "mini-vector" specifying saccade trajectory, and there is a fixed total number of spikes needed to reach a total eye displacement; the overall saccade amplitude is a sum of all of the mini-vectors evoked in the SC at saccade execution. Our results are consistent with this: when the flash appears before saccade triggering, visual spikes would be present in the SC at the time of saccade triggering (Fig. 1), and these spikes would therefore contribute mini-vectors associated with the location of the visual stimulus. This explains why movement amplitude and direction in our experiments "gravitate" toward the center of mass of the location of the visual flash, and it can also account for kinematic alterations. Indeed, this is related to the original motivation for these model: blink-perturbed saccades take much longer to finish but still reach the same eye displacement after the same number of SC spikes is emitted during the movement. Moreover, peak velocity and trajectory of these slow saccades are abnormal and violate the main sequence relationship. According to these mini-vector models, this is because the eye continues to move with each coming mini-vector until movement end, regardless of kinematics (Goossens and Van Opstal 2010). However, these models do invoke a "blink-related" eye movement downstream of the SC (Goossens and Van Opstal 2010), and it would be interesting to know whether an equivalent of this additional movement component exists for flash-affected movements. In the case of microsaccades, we have recently found that frontal eye field (FEF) inactivation upstream of the SC can alter movement kinematics (Peel et al. 2016), but it remains to be understood how FEF input achieves this at the level of the brain stem.

It is also still not clear to us how individual "spikes" in these mini-vector models are "labeled" as contributing a mini-vector for a given movement. For example, if there is low-frequency SC activity in the absence of saccades, what prevents them from contributing an eye movement? In other words, there may be a credit assignment problem in reading SC spikes during and outside saccades, and knowing how the entire final oculomotor output network (i.e., SC and downstream) switches from a "no-saccade" state to a "saccade" state and vice versa would be interesting. For scenarios like in our experiments, if additional visual spikes caused by a flash are read out during a saccade as regular saccade spikes that contribute mini-vectors, then the total number of spikes emitted by the SC could be reached earlier than usual (because of the additional visual spikes). This could in turn cause the early reactivation of OPNs alluded to above and in Fig. 11*B*, *right*, resulting in a combination of spatial readout and interruption effects. It would be interesting to test this potential mechanism experimentally.

Exquisite Control Over Individual Microsaccade Metrics and Kinematics

The fact that we observed kinematic alteration even for the smallest amplitudes (Fig. 8), and even when the flash and movement goal are colocalized (Figs. 5–7), suggests that the oculomotor system can exercise a previously unappreciated and exquisite level of control over individual microsaccades. This adds to the growing list of evidence that microsaccades can play important functional roles (Hafed et al. 2015), and it also explains how microsaccades can precisely relocate the line of sight (Guerrasio et al. 2010; Ko et al. 2010; Poletti et al. 2013; Tian et al. 2016). The neurophysiological implications of such oculomotor system precision are intriguing: on the one hand, the scale of movements to control spans multiple orders of magnitudes, and on the other, the millisecond-by-millisecond evolution of eye trajectory during a single movement is highly malleable and influenced by even individual additional "spikes."

In terms of the former, it would be interesting to contrast the degree to which coarse coding in structures like the SC (Lee et al. 1988) can be sufficient to control tiny eye movements. For large saccades, SC response fields (RFs) are large, suggesting that coarse coding is used to control accurate movement end points (Lee et al. 1988). It has also been proposed that logarithmic warping of eccentricity in SC neural tissue, which entails larger RF sizes for larger eccentricities, can "equalize" the size of the active population of neurons for a wide range of saccade amplitudes (Hafed and Chen 2016; Munoz and Wurtz 1995; Ottes et al. 1986). However, it is still not known how this observation extends into the foveal representation.

In terms of millisecond-by-millisecond movement evolution, the question of microsaccade kinematics remains wide open. Previous work implicates known brain stem areas for saccade control (Van Gisbergen et al. 1981). For example, premotor burst neurons are modulated during microsaccades. However, the data from these early pioneering studies are severely limited from a quantitative perspective; interesting insights could be gleaned if many of these early studies were revisited with more modern techniques for data recording and analysis, and with new perspectives provided by recent behavioral observations.

Having said the above, it is not entirely clear to us why the data of Rolfs et al. (2008) with a foveal flash (as in our Fig. 7)

revealed a decrease in microsaccade amplitudes after the flash, rather than an increase as we saw in our experiments (Fig. 7*A*, second row). Although it is true that they did not separate microsaccade directions in their analyses as we did, the idea that most microsaccades correct for foveal motor errors (e.g., Fig. 5 and Guerrasio et al. 2010; Ko et al. 2010; Poletti et al. 2013; Tian et al. 2016) would predict that most microsaccades in their study would have been toward movements, as in our study. One possibility could be that their task requirements of simple fixation and an irrelevant flash resulted in more evenly distributed microsaccade directions than in our case. Indeed, our monkeys would have lost reward for breaking fixation, meaning that they may have been much more attentive to the task of gaze fixation than human subjects. An additional more likely possibility is that the much larger fixation spot in the Rolfs et al. (2008) study meant that their subjects' gaze was already on the spot most of the time, which would result in flashes that truncate most microsaccades. This is indeed a scenario similar to one of the conditions in the study of Buonocore et al. (2016) for large saccades.

Postinhibition Saccades and Microsaccades

Finally, it would be interesting to explore movements after recovery from saccadic inhibition. These movements, at least for microsaccades, are particularly dependent on a top-down signal from FEF (Peel et al. 2016). Also, data in Fig. 2*D* and the *bottom* row of Fig. 7*A* suggest that postinhibition movements oscillate in amplitude modulations (opposite microsaccades become slightly bigger than towards ones after inhibition). This is reminiscent of post-cue oscillations in microsaccade directions, which reflect an ongoing oscillation in the saccadic system that is unmasked by cue onsets (Hafed and Ignashchenkova 2013; Tian et al. 2016). This might also explain why Fig. 4, *B* and *D*, shows variability in velocity-to-amplitude ratios at different times (e.g., before vs. after stimulus onset for opposite movements in *monkey N*). It would be intriguing to explore whether saccade kinematics may also be governed by ongoing oscillatory brain rhythms (even before flash onset), and what such rhythms might mean for the mechanisms of saccade control.

GRANTS

This work was funded by the Werner Reichardt Centre for Integrative Neuroscience (CIN) at the Eberhard Karls University of Tübingen. The CIN is an Excellence Cluster funded by the Deutsche Forschungsgemeinschaft within the framework of the Excellence Initiative (EXC 307).

DISCLOSURES

No conflicts of interest, financial or otherwise, are declared by the authors.

AUTHOR CONTRIBUTIONS

A.B. and Z.M.H. analyzed data; A.B., C.-Y.C., X.T., and Z.M.H. interpreted results of experiments; A.B. and Z.M.H. prepared figures; A.B. and Z.M.H. drafted manuscript; A.B., C.-Y.C., X.T., and Z.M.H. edited and revised manuscript; A.B., C.-Y.C., X.T., S.I., T.A.M., and Z.M.H. approved final version of manuscript; C.-Y.C., X.T., and Z.M.H. performed experiments.

REFERENCES

Arai K, Das S, Keller EL, Aiyoshi E. A distributed model of the saccade system: simulations of temporally perturbed saccades using position and velocity feedback. *Neural Netw* 12: 1359–1375, 1999. doi:10.1016/S0893-6080(99)00077-5.

Arnstein D, Junker M, Smilgin A, Dicke PW, Thier P. Microsaccade control signals in the cerebellum. *J Neurosci* 35: 3403–3411, 2015. doi:10.1523/JNEUROSCI.2458-14.2015.

Bahill AT, Clark MR, Stark L. The main sequence, a tool for studying human eye movements. *Math Biosci* 24: 191–204, 1975. doi:10.1016/0025-5564(75)90075-9.

Bompas A, Sumner P. Saccadic inhibition reveals the timing of automatic and voluntary signals in the human brain. *J Neurosci* 31: 12501–12512, 2011. doi:10.1523/JNEUROSCI.2234-11.2011.

Buonocore A, McIntosh RD. Saccadic inhibition underlies the remote distractor effect. *Exp Brain Res* 191: 117–122, 2008. doi:10.1007/s00221-008-1558-7.

Buonocore A, McIntosh RD. Modulation of saccadic inhibition by distractor size and location. *Vision Res* 69: 32–41, 2012. doi:10.1016/j.visres.2012.07.010.

Buonocore A, McIntosh RD, Melcher D. Beyond the point of no return: effects of visual distractors on saccade amplitude and velocity. *J Neurophysiol* 115: 752–762, 2016. doi:10.1152/jn.00939.2015.

Büttner-Ennever JA, Horn AKE, Henn V, Cohen B. Projections from the superior colliculus motor map to omnipause neurons in monkey. *J Comp Neurol* 413: 55–67, 1999. doi:10.1002/(SICI)1096-9861(19991011)413:1<55::AID-CNE3>3.0.CO;2-K.

Chen CY, Hafed ZM. Postmicrosaccadic enhancement of slow eye movements. *J Neurosci* 33: 5375–5386, 2013. doi:10.1523/JNEUROSCI.3703-12.2013.

Chen CY, Hafed ZM. A neural locus for spatial-frequency specific saccadic suppression in visual-motor neurons of the primate superior colliculus. *J Neurophysiol* 2016, 2017. doi:10.1152/jn.00911.2016.

Chen CY, Ignashchenkova A, Thier P, Hafed ZM. Neuronal response gain enhancement prior to microsaccades. *Curr Biol* 25: 2065–2074, 2015. doi:10.1016/j.cub.2015.06.022.

Dorris MC, Olivier E, Munoz DP. Competitive integration of visual and preparatory signals in the superior colliculus during saccadic programming. *J Neurosci* 27: 5053–5062, 2007. doi:10.1523/JNEUROSCI.4212-06.2007.

Edelman JA, Xu KZ. Inhibition of voluntary saccadic eye movement commands by abrupt visual onsets. *J Neurophysiol* 101: 1222–1234, 2009. doi:10.1152/jn.90708.2008.

Engbert R, Kliegl R. Microsaccades uncover the orientation of covert attention. *Vision Res* 43: 1035–1045, 2003. doi:10.1016/S0042-6989(03)00084-1.

Everling S, Paré M, Dorris MC, Munoz DP. Comparison of the discharge characteristics of brain stem omnipause neurons and superior colliculus fixation neurons in monkey: implications for control of fixation and saccade behavior. *J Neurophysiol* 79: 511–528, 1998.

Findlay JM. Global visual processing for saccadic eye movements. *Vision Res* 22: 1033–1045, 1982. doi:10.1016/0042-6989(82)90040-2.

Findlay JM, Harris LR. Small saccades to double-stepped targets moving in two dimensions. In: *Theoretical and Applied Aspects of Eye Movement Research*, edited by Gale AG and Johnson F. Amsterdam: North-Holland, 1984, p. 71–78. doi:10.1016/S0166-4115(08)61820-8.

Findlay JM, Walker R. A model of saccade generation based on parallel processing and competitive inhibition. *Behav Brain Sci* 22: 661–674, 1999. doi:10.1017/S0140525X99002150.

Gandhi NJ, Keller EL. Spatial distribution and discharge characteristics of superior colliculus neurons antidromically activated from the omnipause region in monkey. *J Neurophysiol* 78: 2221–2225, 1997.

Goossens HH, Van Opstal AJ. Differential effects of reflex blinks on saccade perturbations in humans. *J Neurophysiol* 103: 1685–1695, 2010. doi:10.1152/jn.00788.2009.

Goossens HH, van Opstal AJ. Optimal control of saccades by spatial-temporal activity patterns in the monkey superior colliculus. *PLoS Comput Biol* 8: e1002508, 2012. doi:10.1371/journal.pcbi.1002508.

Graupner S-T, Velichkovsky BM, Pannasch S, Marx J. Surprise, surprise: two distinct components in the visually evoked distractor effect. *Psychophysiology* 44: 251–261, 2007. doi:10.1111/j.1469-8986.2007.00504.x.

Guerrasio L, Quinet J, Büttner U, Goffart L. Fastigial oculomotor region and the control of foveation during fixation. *J Neurophysiol* 103: 1988–2001, 2010. doi:10.1152/jn.00771.2009.

Guillaume A. Saccadic inhibition is accompanied by large and complex amplitude modulations when induced by visual backward masking. *J Vis* 12: 5, 2012. doi:10.1167/12.6.5.

Hafed ZM. Mechanisms for generating and compensating for the smallest possible saccades. *Eur J Neurosci* 33: 2101–2113, 2011. doi:10.1111/j.1460-9568.2011.07694.x.

Hafed ZM. Alteration of visual perception prior to microsaccades. *Neuron* 77: 775–786, 2013. doi:10.1016/j.neuron.2012.12.014.

Hafed ZM. Saccades and smooth pursuit eye movements. In: *From Neuron to Cognition via Computational Neuroscience*, edited by Arbib MA and Bonaiuto JJ. Cambridge, MA: MIT Press, 2016, p. 559–584.

Hafed ZM, Chen CY. Sharper, stronger, faster upper visual field representation in primate superior colliculus. *Curr Biol* 26: 1647–1658, 2016. doi:10.1016/j.cub.2016.04.059.

Hafed ZM, Chen CY, Tian X. Vision, perception, and attention through the lens of microsaccades: mechanisms and implications. *Front Syst Neurosci* 9: 167, 2015. doi:10.3389/fnsys.2015.00167.

Hafed ZM, Clark JJ. Microsaccades as an overt measure of covert attention shifts. *Vision Res* 42: 2533–2545, 2002. doi:10.1016/S0042-6989(02)00263-8.

Hafed ZM, Goffart L, Krauzlis RJ. A neural mechanism for microsaccade generation in the primate superior colliculus. *Science* 323: 940–943, 2009. doi:10.1126/science.1166112.

Hafed ZM, Ignashchenkova A. On the dissociation between microsaccade rate and direction after peripheral cues: microsaccadic inhibition revisited. *J Neurosci* 33: 16220–16235, 2013. doi:10.1523/JNEUROSCI.2240-13.2013.

Hafed ZM, Krauzlis RJ. Microsaccadic suppression of visual bursts in the primate superior colliculus. *J Neurosci* 30: 9542–9547, 2010. doi:10.1523/JNEUROSCI.1137-10.2010.

Hafed ZM, Krauzlis RJ. Similarity of superior colliculus involvement in microsaccade and saccade generation. *J Neurophysiol* 107: 1904–1916, 2012. doi:10.1152/jn.01125.2011.

Hafed ZM, Lovejoy LP, Krauzlis RJ. Modulation of microsaccades in monkey during a covert visual attention task. *J Neurosci* 31: 15219–15230, 2011. doi:10.1523/JNEUROSCI.3106-11.2011.

Hafed ZM, Lovejoy LP, Krauzlis RJ. Superior colliculus inactivation alters the relationship between covert visual attention and microsaccades. *Eur J Neurosci* 37: 1169–1181, 2013. doi:10.1111/ejn.12127.

Hartwich-Young R, Nelson JS, Sparks DL. The perihypoglossal projection to the superior colliculus in the rhesus monkey. *Vis Neurosci* 4: 29–42, 1990. doi:10.1017/S0952523800002741.

Katnani HA, Gandhi NJ. Time course of motor preparation during visual search with flexible stimulus-response association. *J Neurosci* 33: 10057–10065, 2013. doi:10.1523/JNEUROSCI.0850-13.2013.

Katnani HA, Van Opstal AJ, Gandhi NJ. A test of spatial temporal decoding mechanisms in the superior colliculus. *J Neurophysiol* 107: 2442–2452, 2012. doi:10.1152/jn.00992.2011.

Katnani HA, Van Opstal AJ, Gandhi NJ. Blink perturbation effects on saccades evoked by microstimulation of the superior colliculus. *PLoS One* 7: e51843, 2012b. doi:10.1371/journal.pone.0051843.

Keller EL. Participation of medial pontine reticular formation in eye movement generation in monkey. *J Neurophysiol* 37: 316–332, 1974.

Keller EL, Edelman JA. Use of interrupted saccade paradigm to study spatial and temporal dynamics of saccadic burst cells in superior colliculus in monkey. *J Neurophysiol* 72: 2754–2770, 1994.

Ko HK, Poletti M, Rucci M. Microsaccades precisely relocate gaze in a high visual acuity task. *Nat Neurosci* 13: 1549–1553, 2010. doi:10.1038/nn.2663.

Lee C, Rohrer WH, Sparks DL. Population coding of saccadic eye movements by neurons in the superior colliculus. *Nature* 332: 357–360, 1988. doi:10.1038/332357a0.

Ludwig CJ, Mildinhall JW, Gilchrist ID. A population coding account for systematic variation in saccadic dead time. *J Neurophysiol* 97: 795–805, 2007. doi:10.1152/jn.00652.2006.

McPeek RM, Han JH, Keller EL. Competition between saccade goals in the superior colliculus produces saccade curvature. *J Neurophysiol* 89: 2577–2590, 2003. doi:10.1152/jn.00657.2002.

Mégardon G, Tandonnet C, Sumner P, Guillaume A. Limitations of short range Mexican hat connection for driving target selection in a 2D neural field: activity suppression and deviation from input stimuli. *Front Comput Neurosci* 9: 128, 2015. doi:10.3389/fncom.2015.00128.

Missal M, Keller EL. Common inhibitory mechanism for saccades and smooth-pursuit eye movements. *J Neurophysiol* 88: 1880–1892, 2002.

Moschovakis AK, Scudder CA, Highstein SM. The microscopic anatomy and physiology of the mammalian saccadic system. *Prog Neurobiol* 50: 133–254, 1996. doi:10.1016/S0301-0082(96)00034-2.

Munoz DP, Wurtz RH. Saccade-related activity in monkey superior colliculus. II. Spread of activity during saccades. *J Neurophysiol* 73: 2334–2348, 1995.

Ottes FP, Van Gisbergen JA, Eggermont JJ. Visuomotor fields of the superior colliculus: a quantitative model. *Vision Res* 26: 857–873, 1986. doi:10.1016/0042-6989(86)90144-6.

Pannasch S, Dornhoefer SM, Unema PJA, Velichkovsky BM. The omnipresent prolongation of visual fixations: saccades are inhibited by changes in situation and in subject's activity. *Vision Res* 41: 3345–3351, 2001. doi:10.1016/S0042-6989(01)00207-3.

Peel TR, Hafed ZM, Dash S, Lomber SG, Corneil BD. A Causal Role for the Cortical Frontal Eye Fields in Microsaccade Deployment. *PLoS Biol* 14: e1002531, 2016. doi:10.1371/journal.pbio.1002531.

Poletti M, Listorti C, Rucci M. Microscopic eye movements compensate for nonhomogeneous vision within the fovea. *Curr Biol* 23: 1691–1695, 2013. doi:10.1016/j.cub.2013.07.007.

Reingold EM, Stampe DM. Saccadic inhibition in complex visual tasks. In: *Current Oculomotor Research*, edited by Becker W, Deubel H, and Mergner T. Boston: Springer, 1999, p. 249–255. doi:10.1007/978-1-4757-3054-8_35.

Reingold EM, Stampe DM. Saccadic inhibition and gaze contingent research paradigms. In: Reading as a Perceptual Process, edited by Kennedy A, Radach R, Heller D, and Pynte J. Amsterdam: North-Holland, 2000, p. 119–145.

Reingold EM, Stampe DM. Saccadic inhibition in voluntary and reflexive saccades. *J Cogn Neurosci* 14: 371–388, 2002. doi:10.1162/089892902317361903.

Reingold EM, Stampe DM. Saccadic inhibition in reading. *J Exp Psychol Hum Percept Perform* 30: 194–211, 2004. doi:10.1037/0096-1523.30.1.194.

Rolfs M, Kliegl R, Engbert R. Toward a model of microsaccade generation: the case of microsaccadic inhibition. *J Vis* 8: 5.1–5.23, 2008. doi:10.1167/8.11.5.

Rottach KG, Das VE, Wohlgemuth W, Zivotofsky AZ, Leigh RJ. Properties of horizontal saccades accompanied by blinks. *J Neurophysiol* 79: 2895–2902, 1998.

Schultz KP, Williams CR, Busettini C. Macaque pontine omnipause neurons play no direct role in the generation of eye blinks. *J Neurophysiol* 103: 2255–2274, 2010. doi:10.1152/jn.01150.2009.

Scudder CA, Kaneko CS, Fuchs AF. The brainstem burst generator for saccadic eye movements: a modern synthesis. *Exp Brain Res* 142: 439–462, 2002. doi:10.1007/s00221-001-0912-9.

Strassman A, Evinger C, McCrea RA, Baker RG, Highstein SM. Anatomy and physiology of intracellularly labelled omnipause neurons in the cat and squirrel monkey. *Exp Brain Res* 67: 436–440, 1987. doi:10.1007/BF00248565.

Tian X, Yoshida M, Hafed ZM. A microsaccadic account of attentional capture and inhibition of return in Posner cueing. *Front Syst Neurosci* 10: 23, 2016. doi:10.3389/fnsys.2016.00023.

Van Gisbergen JA, Robinson DA, Gielen S. A quantitative analysis of generation of saccadic eye movements by burst neurons. *J Neurophysiol* 45: 417–442, 1981.

Walker R, Deubel H, Schneider WX, Findlay JM. Effect of remote distractors on saccade programming: evidence for an extended fixation zone. *J Neurophysiol* 78: 1108–1119, 1997.

Zuber BL, Stark L, Cook G. Microsaccades and the velocity-amplitude relationship for saccadic eye movements. *Science* 150: 1459–1460, 1965. doi:10.1126/science.150.3702.1459.